

Motion and Radiation of Binary Black Holes: the Effective-One-Body Approach

Thibault Damour

Institut des Hautes Etudes Scientifiques (Bures-sur-Yvette, France)



Basic Effective-One-Body (EOB) formalism: Buonanno Damour 1999,2000;
Damour Jaranowski Schäfer, 2000;
Damour, 2001

Developments of EOB formalism: Damour Gopakumar 2006;
Buonanno Chen Damour 2006;
Damour Nagar 2007a, 2007b
Damour Jaranowski Schäfer 2008
Damour Iyer Nagar 2008

Comparisons to NR data: Buonanno Cook Pretorius 2007
Damour Nagar 2007a, 2007b, 2007c
Pan et al. 2008
Buonanno, Pan, Baker et al. 2007
Damour Nagar Dorband et al. 2007
Damour Nagar Hannam et al. 2008
Boyle Buonanno et al. 2008

BBH: A premier source for detectors of Gravitational Waves (GW)

A network of ground-based interferometric gravitational wave (GW) detectors (LIGO/VIRGO/GEO) is now taking data near its planned sensitivity.

Coalescing (stellar-mass, $M \sim 30M_{\text{sun}}$) binary black hole systems (BBHs) are among the most promising GW sources for these detectors.

Most useful part of the waveform is emitted in **the last 5 orbits** of the inspiral and during the plunge that takes place after the crossing of the Last Stable Orbit (LSO).

To successfully detect GWs from BBHs coalescence one **needs to know in advance the shape of the signal**

Detection and data analysis is made by means of **templates** that accurately represent the gravitational waveforms emitted by the source.

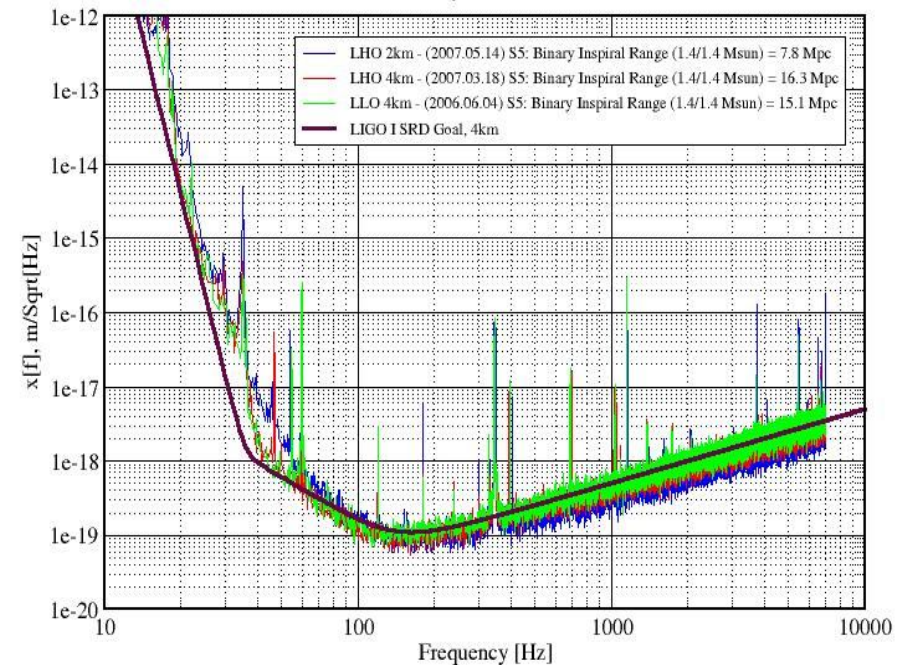
State-of-the art Numerical Relativity (NR) simulations can now merge black-holes, but are not sufficiently efficient to densely sample the parameter space.

One needs analytical methods to produce thousands of templates (possibly in real time)



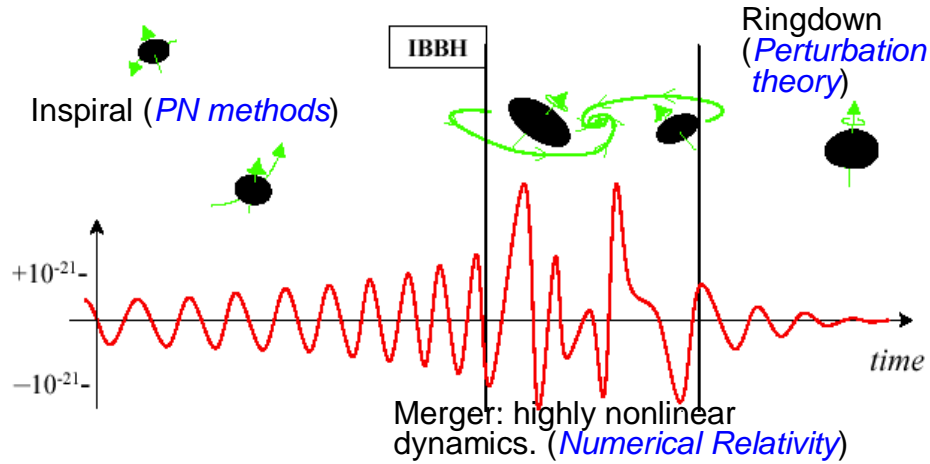
Displacement Sensitivity of the LIGO Interferometers

Performance for S5 - May 2007 LIGO-G070367-00-E

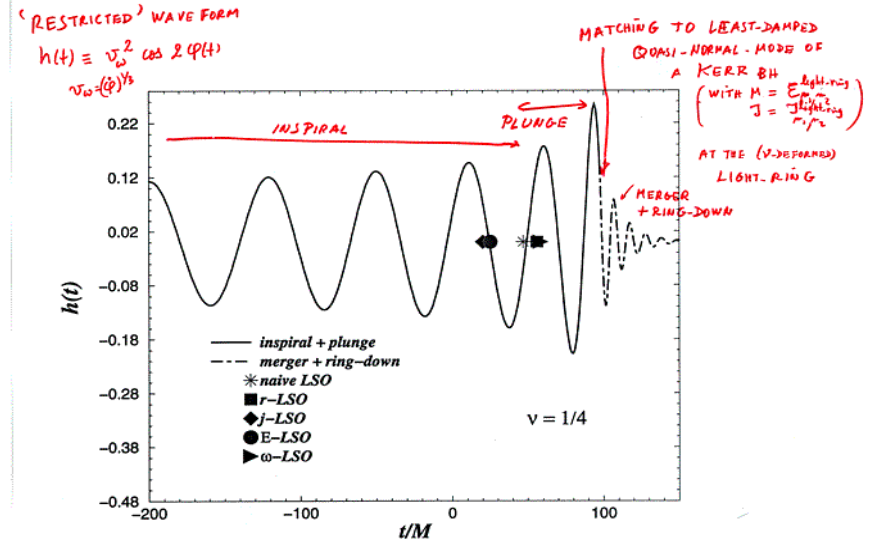


Templates for GWs from BBH coalescence

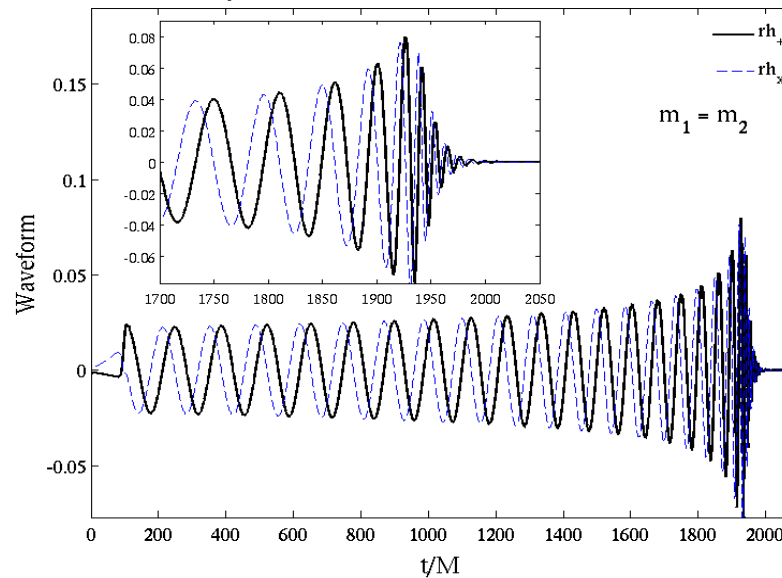
(Brady, Craighton, Thorne 1998)



(Buonanno & Damour 1999)



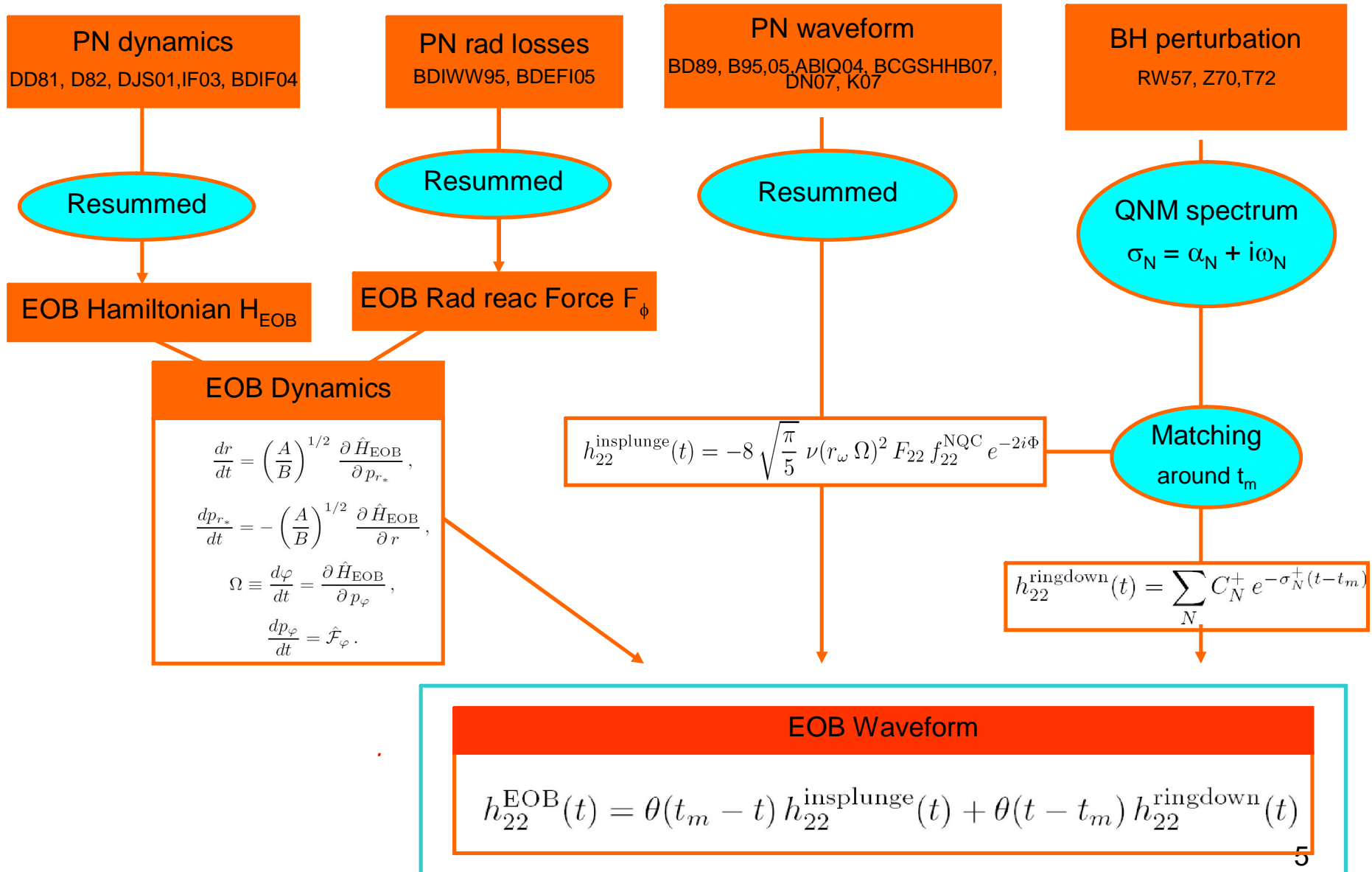
Numerical Relativity, the 2005 breakthrough:
Pretorius, Campanelli et al., Baker et al. ...



Aim of the Effective-One-Body (EOB) formalism

- To provide an *accurate analytical* description of the motion and radiation of binary black holes, which covers inspiral, plunge, merger and ringdown
- Idea: to extend the domain of validity of perturbation theory (PN, BH-pert) so as to approximately cover non-perturbative features
- (Expected) Utility of EOB formalism:
 - provide accurate GW templates for the multi-parameter space $(m_1, m_2, \mathbf{S}_1, \mathbf{S}_2, \dots)$ which is difficult to densely cover with NR
 - gives us a physical understanding of dynamics and radiation
 - can be extended to BH-NS or NS-NS systems up to tidal disruption.

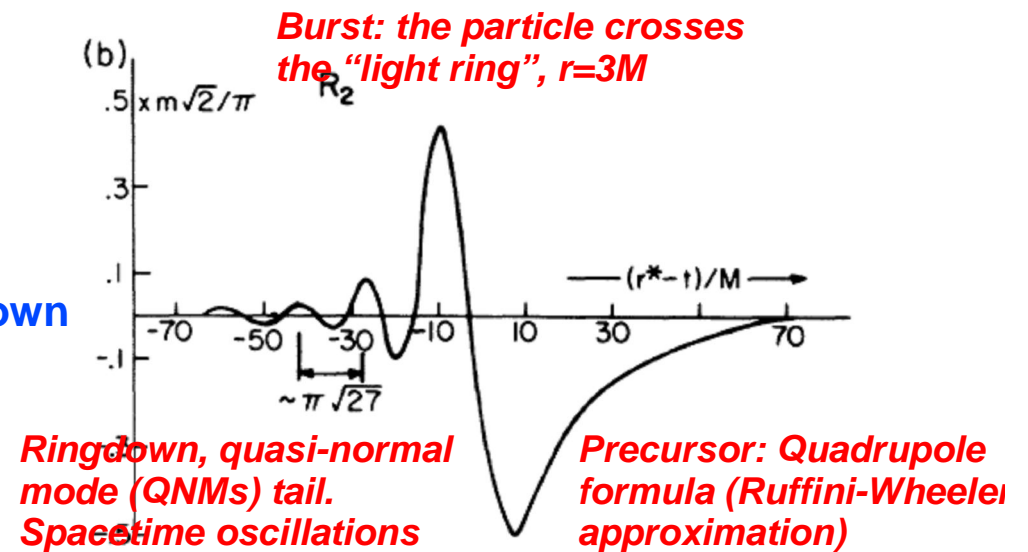
Structure of EOB formalism



Historical roots of EOB

- H_{EOB} : Quantum Hamiltonian $H(I_a)$ [Sommerfeld 1916, Damour-Schäfer 1988]
QED positronium states [Brezin, Itzykson, Zinn-Justin 1970]
- F_ϕ : Padé resummation [DIS 1998]
- $h(t)$: [Davis, Ruffini, Tiomno 1972]
CLAP [Price-Pullin 1994]

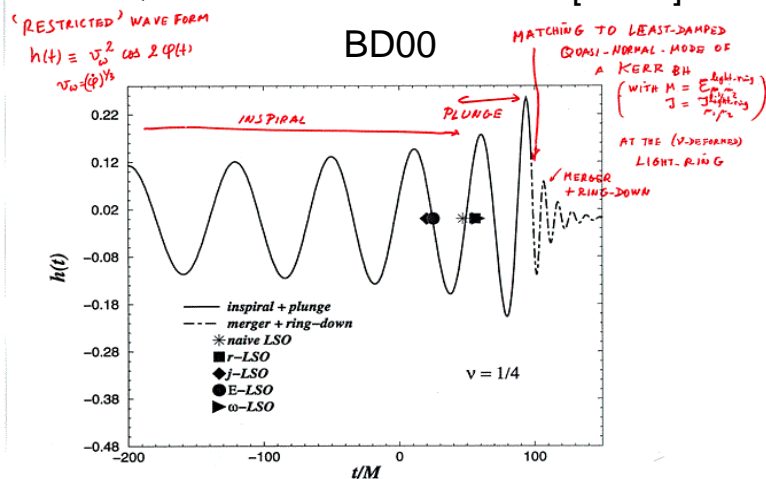
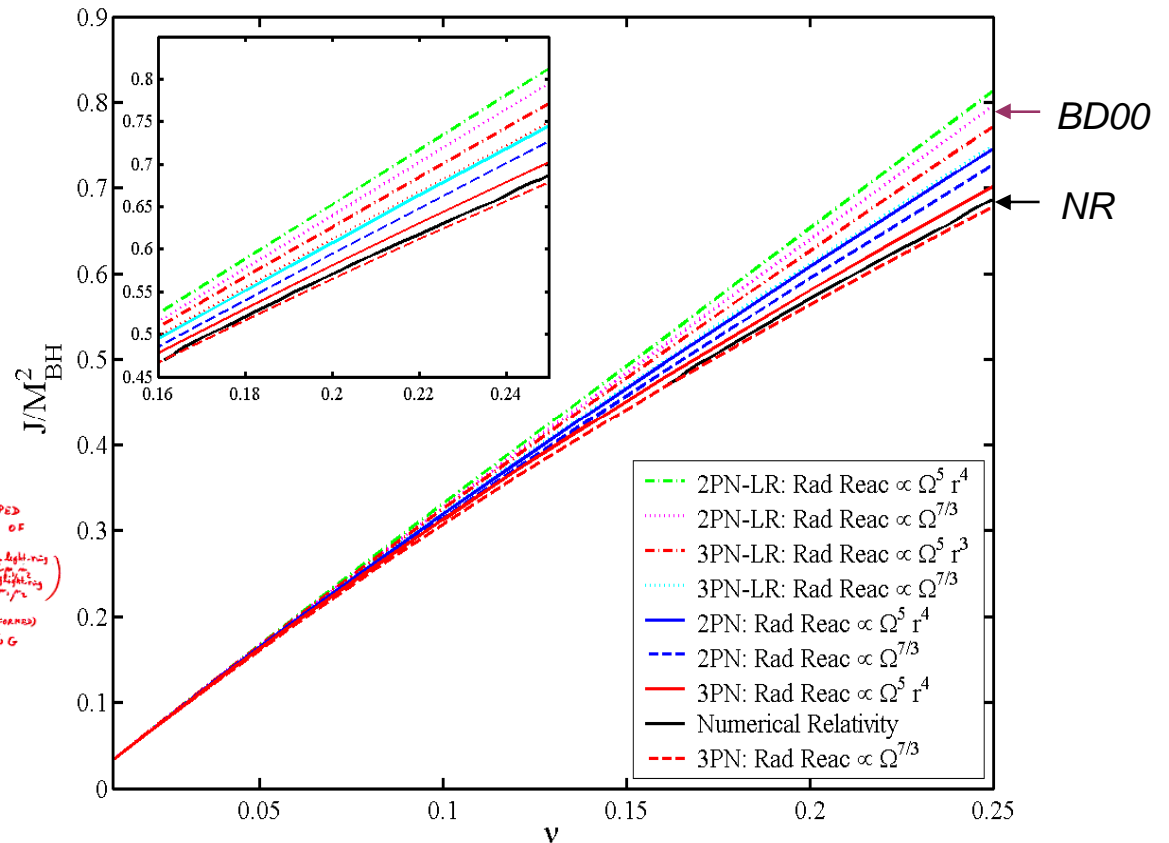
Discovery of the structure:
Precursor (plunge)-Burst (merger)-Ringdown



Successful predictions from EOB

- i. Importance of nonadiabatic effects at the end of inspiral
- ii. Blurred transition from inspiral to a “plunge” that is just a smooth continuation of the inspiral
- iii. First estimate of a complete GW waveform [BD00]
- iv. Estimates of the radiated energy and of the spin of the final black hole, e.g. $J/M^2 \sim 0.795$ [2PN, LSO, BD00]; 0.77 [3PN, >LSO, BCD06]
- v. Parallel spins imply larger radiated energy (tighter orbits), and $J/M^2 < 1$ [D01,BCD06]
- vi. Qualitative recoil versus time [DG06]

Damour, Nagar, PRD **76**, 044003 (2007)

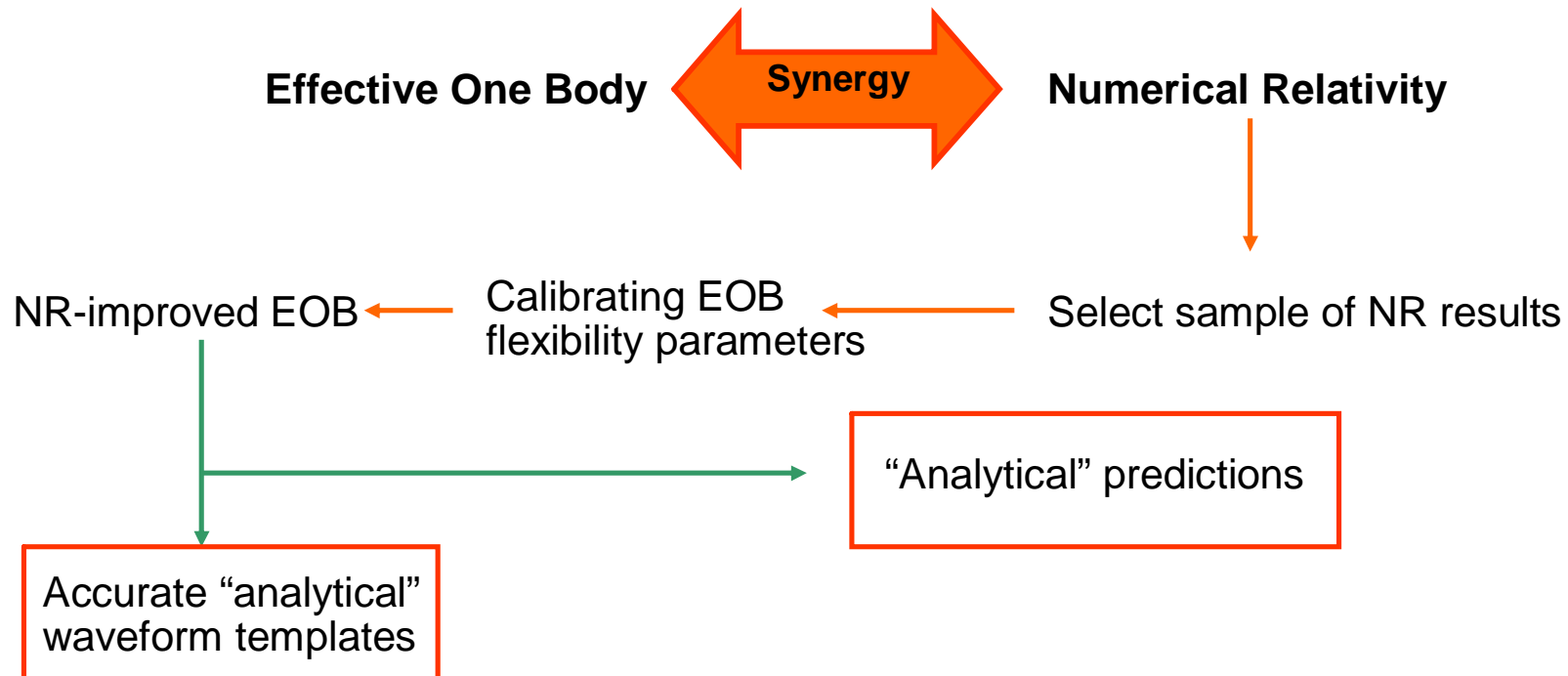


Flexibility of EOB

However, the EOB approach, far from being a rigid structure, is extremely flexible. One can modify the basic functions [such as $A(u)$] determining the EOB dynamics by introducing new parameters corresponding to (yet) uncalculated higher PN effects. [These terms become important only for orbits closer than $6GM$, and/or for fast-spinning holes.] Therefore, when either higher-accuracy analytical calculations are performed or numerical relativity becomes able to give physically relevant data about the interaction of (fast-spinning) black holes, we expect that it will be possible to complete the current EOB Hamiltonian so as to incorporate this information. As the parameter space of two spinning black holes (with arbitrarily oriented spins) is very large, numerical relativity will never be able, by itself, to cover it densely. We think, however, that a suitable “numerically fitted” (and, if possible, “analytically extended”) EOB Hamiltonian should be able to fit the needs of upcoming GW detectors. (Damour 2001)

EOB flexibility parameters

- a_5 [a.k.a. $a_5(v)$, b_5 , λ , a_5^1](D01, DGG02)
- v_{pole} , a_{RR}, \dots (DIJS03)
- a, b : non-quasi-circular corrections to waveform (DN07a, DN07b)
- p, δ : matching “comb” (DN07a)



Defining H_{EOB} by thinking quantum-mechanically (Wheeler)

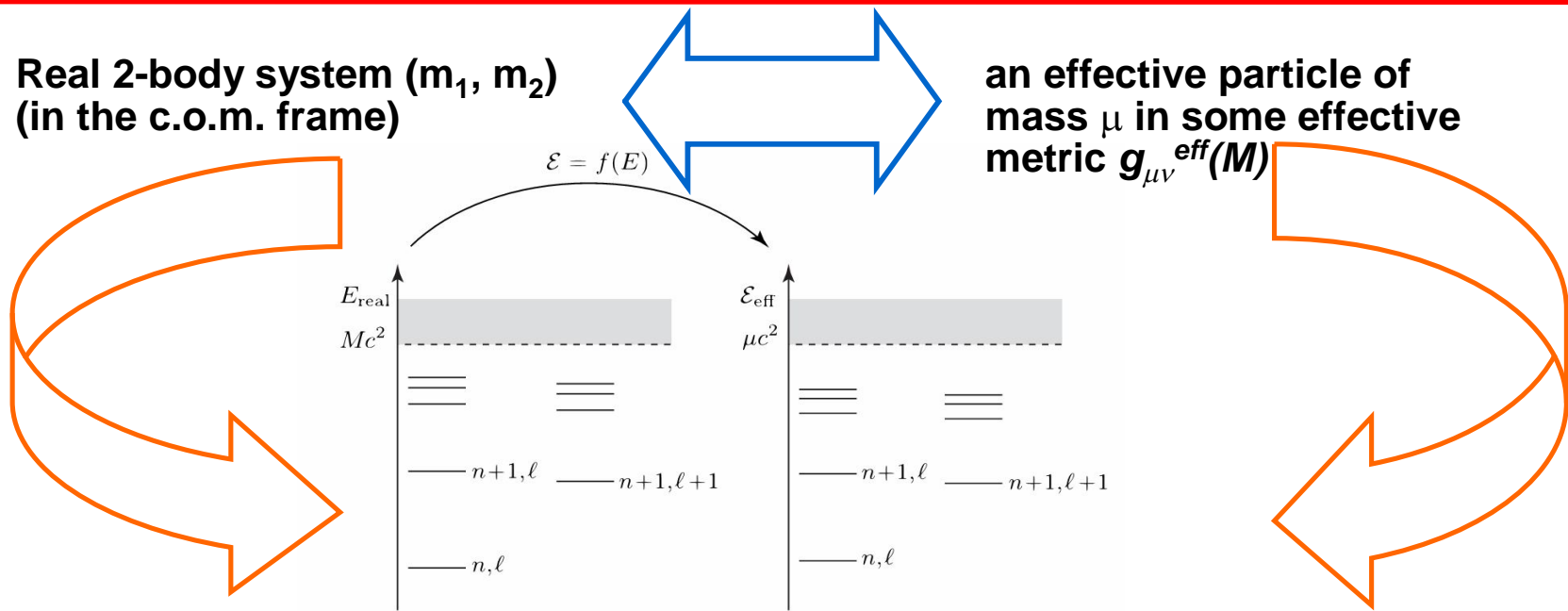


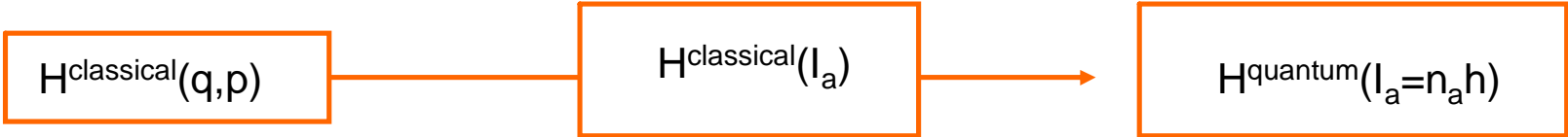
Figure 1: Sketch of the correspondence between the quantized energy levels of the real and effective conservative dynamics. n denotes the ‘principal quantum

Sommerfeld “Old Quantum Mechanics”:

$$J = \ell \hbar = \frac{1}{2\pi} \oint p_\varphi d\varphi$$

$$N = n \hbar = I_r + J$$

$$I_r = \frac{1}{2\pi} \oint p_r dr = I_r + J$$



Damour, Schäfer '88
 Damour, Jaranowski, Schäfer, '00

The 2-body Hamiltonian [at 2PN for clarity]

The 2-body Hamiltonian in the c.o.m frame at 2PN:

$$H_{2\text{PN}}^{\text{relative}}(\mathbf{q}, \mathbf{p}) = H_0(\mathbf{q}, \mathbf{p}) + \frac{1}{c^2} H_2(\mathbf{q}, \mathbf{p}) + \frac{1}{c^4} H_4(\mathbf{q}, \mathbf{p})$$

The Newtonian limit :

$$H_0(\mathbf{q}, \mathbf{p}) = \frac{1}{2\mu} \mathbf{p}^2 + \frac{GM\mu}{|\mathbf{q}|}$$

4 additional terms at 1PN

7 additional terms at 2PN

11 additional terms at 3PN

Rewrite the c.o.m. energy using *action variables* (à la Sommerfeld):
obtain the “quantum” energy levels [from Damour&Schaefer 1988]

$$E_{2\text{PN}}^{\text{relative}}(n, \ell) = -\frac{1}{2} \mu \frac{\alpha^2}{n^2} \left[1 + \frac{\alpha^2}{c^2} \left(\frac{c_{11}}{n\ell} + \frac{c_{20}}{n^2} \right) + \frac{\alpha^4}{c^4} \left(\frac{c_{13}}{n\ell^3} + \frac{c_{22}}{n^2\ell^2} + \frac{c_{31}}{n^3\ell} + \frac{c_{40}}{n^4} \right) \right]$$

“Balmer” formula

“*Delaunay Hamiltonian*”

■ Dependence on $\nu \equiv \mu/M$

■ PN correction: open orbits

■ Degeneracy removed

$$J = \ell \hbar = \frac{1}{2\pi} \oint p_\varphi d\varphi$$

$$N = n \hbar = I_r + J$$

$$I_r = \frac{1}{2\pi} \oint p_r dr$$

$$\alpha \equiv GM\mu/\hbar = G m_1 m_2/\hbar$$

Dictionary between real and effective dynamics

- Unknowns: $\mu, M, f(E), g_{\mu\nu}^{\text{eff}}(M) + \text{Finslerian corrections}$

$$ds^2 = -A(r)dt^2 + B(r)dr^2 + r^2(d\theta^2 + \sin^2\theta d\varphi^2).$$

$$A(R) = 1 + a_1 \frac{GM}{c^2 R} + a_2 \left(\frac{GM}{c^2 R}\right)^2 + a_3 \left(\frac{GM}{c^2 R}\right)^3 + \dots;$$

$$B(R) = 1 + b_1 \frac{GM}{c^2 R} + b_2 \left(\frac{GM}{c^2 R}\right)^2 + \dots,$$

- Dictionary:

$$I_a^{\text{real}} = I_a^{\text{effective}}$$

$$M = m_1 + m_2$$

$$\mu = m_1 m_2 / M$$

$$\nu \equiv m_1 m_2 / M^2$$

$$\frac{\mathcal{E}_{\text{eff}}}{\mu c^2} = 1 + \frac{E_{\text{real}}^{\text{relative}}}{\mu c^2} \left(1 + \frac{\nu}{2} \frac{E_{\text{real}}^{\text{relative}}}{\mu c^2} \right)$$

Explicit form of the effective metric

The effective metric at 3PN + a 4PN correction

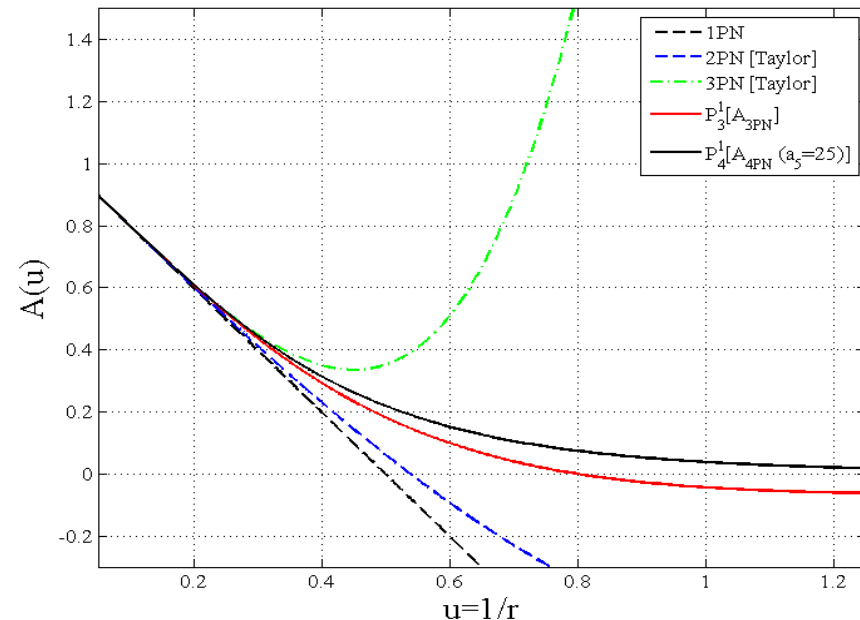
$$ds^2 = -A(r)dt^2 + B(r)dr^2 + r^2(d\theta^2 + \sin^2\theta d\varphi^2).$$

where the coefficients are a ν -dependent “deformation” of the Schwarzschild ones:

$$(BA)^{3\text{PN}}(r) \equiv D^{3\text{PN}}(r) \equiv 1 - \frac{6\nu}{r^2} + 2(3\nu - 26)\frac{\nu}{r^3}.$$

$$A^{\text{Taylor}}(u) = 1 - 2u + 2\nu u^3 + \left(\frac{94}{3} - \frac{41}{32}\pi^2\right)\nu u^4 + a_5\nu u^5 + \mathcal{O}(\nu u^6), \quad u = 1/r$$

- Extremely compact representation of PN dynamics
- Bad behaviour at 3PN. Padé resummation of $A(r)$ is needed to ensure that an effective horizon exists.
- Impose, by continuity with the Schwarzschild case, that $A(r)$ has a simple zero at $r=2$.
- The a_5 constant parametrizes (yet) uncalculated 4PN corrections



2-body Taylor-expanded 3PN Hamiltonian [Damour, Jaranowski, Schäfer, 01]

$$H(\mathbf{x}_a, \mathbf{p}_a) = \sum_a m_a c^2 + H_N(\mathbf{x}_a, \mathbf{p}_a) + \frac{1}{c^2} H_{1\text{PN}}(\mathbf{x}_a, \mathbf{p}_a) + \frac{1}{c^4} H_{2\text{PN}}(\mathbf{x}_a, \mathbf{p}_a) + \frac{1}{c^6} H_{3\text{PN}}(\mathbf{x}_a, \mathbf{p}_a) + \mathcal{O}\left(\frac{1}{c^8}\right)$$

$$H_N(\mathbf{x}_a, \mathbf{p}_a) = \sum_a \frac{\mathbf{p}_a^2}{2m_a} - \frac{1}{2} \sum_a \sum_{b \neq a} \frac{G m_a m_b}{r_{ab}}$$

$$H_{1\text{PN}}(\mathbf{x}_a, \mathbf{p}_a) = -\frac{1}{8} \frac{(\mathbf{p}_1^2)^2}{m_1^3} + \frac{1}{8} \frac{G m_1 m_2}{r_{12}} \left[-12 \frac{\mathbf{p}_1^2}{m_1^2} + 14 \frac{(\mathbf{p}_1 \cdot \mathbf{p}_2)}{m_1 m_2} + 2 \frac{(\mathbf{n}_{12} \cdot \mathbf{p}_1)(\mathbf{n}_{12} \cdot \mathbf{p}_2)}{m_1 m_2} \right] + \frac{1}{4} \frac{G m_1 m_2}{r_{12}} \frac{G(m_1 + m_2)}{r_{12}} + (1 \leftrightarrow 2), \quad 1\text{PN}$$

$$H_{2\text{PN}}(\mathbf{x}_a, \mathbf{p}_a) = \frac{1}{16} \frac{(\mathbf{p}_1^2)^3}{m_1^5} + \frac{1}{8} \frac{G m_1 m_2}{r_{12}} \left[5 \frac{(\mathbf{p}_1^2)^2}{m_1^3} - \frac{11}{2} \frac{\mathbf{p}_1^2 \mathbf{p}_2^2}{m_1^2 m_2^2} - \frac{(\mathbf{p}_1 \cdot \mathbf{p}_2)^2}{m_1^2 m_2^2} + 5 \frac{\mathbf{p}_1^2 (\mathbf{n}_{12} \cdot \mathbf{p}_2)^2}{m_1^2 m_2^2} \right. \\ \left. - 6 \frac{(\mathbf{p}_1 \cdot \mathbf{p}_2)(\mathbf{n}_{12} \cdot \mathbf{p}_1)(\mathbf{n}_{12} \cdot \mathbf{p}_2)}{m_1^2 m_2^2} - \frac{3}{2} \frac{(\mathbf{n}_{12} \cdot \mathbf{p}_1)^2 (\mathbf{n}_{12} \cdot \mathbf{p}_2)^2}{m_1^2 m_2^2} \right] \\ + \frac{1}{4} \frac{G^2 m_1 m_2}{r_{12}^2} \left[m_2 \left(10 \frac{\mathbf{p}_1^2}{m_1^2} + 19 \frac{\mathbf{p}_2^2}{m_2^2} \right) - \frac{1}{2} (m_1 + m_2) \frac{27 (\mathbf{p}_1 \cdot \mathbf{p}_2) + 6 (\mathbf{n}_{12} \cdot \mathbf{p}_1)(\mathbf{n}_{12} \cdot \mathbf{p}_2)}{m_1 m_2} \right] \\ - \frac{1}{8} \frac{G m_1 m_2}{r_{12}} \frac{G^2 (m_1^2 + 5 m_1 m_2 + m_2^2)}{r_{12}^2} + (1 \leftrightarrow 2).$$

2PN

$$H_{3\text{PN}}^{\text{reg}}(\mathbf{x}_a, \mathbf{p}_a) = -\frac{5}{128} \frac{(\mathbf{p}_1^2)^4}{m_1^5} + \frac{1}{32} \frac{G m_1 m_2}{r_{12}} \left[-14 \frac{(\mathbf{p}_1^2)^3}{m_1^3} + 4 \frac{(\mathbf{p}_1 \cdot \mathbf{p}_2)^2 + 4 \mathbf{p}_1^2 \mathbf{p}_2^2}{m_1^2 m_2^2} \mathbf{p}_1^2 + \frac{(\mathbf{p}_1^2 \mathbf{p}_2^2 - 2 (\mathbf{p}_1 \cdot \mathbf{p}_2)^2)(\mathbf{p}_1 \cdot \mathbf{p}_2)}{m_1^2 m_2^2} \right. \\ \left. - 10 \frac{(\mathbf{p}_1^2 (\mathbf{n}_{12} \cdot \mathbf{p}_2)^2 + \mathbf{p}_2^2 (\mathbf{n}_{12} \cdot \mathbf{p}_1)^2) \mathbf{p}_1^2}{m_1^2 m_2^2} + 24 \frac{\mathbf{p}_1^2 (\mathbf{p}_1 \cdot \mathbf{p}_2)(\mathbf{n}_{12} \cdot \mathbf{p}_1)(\mathbf{n}_{12} \cdot \mathbf{p}_2)}{m_1^2 m_2^2} + 2 \frac{\mathbf{p}_1^2 (\mathbf{p}_1 \cdot \mathbf{p}_2)(\mathbf{n}_{12} \cdot \mathbf{p}_2)^2}{m_1^2 m_2^2} \right. \\ \left. + \frac{7 \mathbf{p}_1^2 \mathbf{p}_2^2 - 10 (\mathbf{p}_1 \cdot \mathbf{p}_2)^2}{m_1^2 m_2^2} (\mathbf{n}_{12} \cdot \mathbf{p}_1)(\mathbf{n}_{12} \cdot \mathbf{p}_2) + 6 \frac{\mathbf{p}_1^2 (\mathbf{n}_{12} \cdot \mathbf{p}_1)^2 (\mathbf{n}_{12} \cdot \mathbf{p}_2)^2}{m_1^2 m_2^2} \right. \\ \left. + 15 \frac{(\mathbf{p}_1 \cdot \mathbf{p}_2)(\mathbf{n}_{12} \cdot \mathbf{p}_1)^2 (\mathbf{n}_{12} \cdot \mathbf{p}_2)^2}{m_1^2 m_2^2} - 18 \frac{\mathbf{p}_1^2 (\mathbf{n}_{12} \cdot \mathbf{p}_1)(\mathbf{n}_{12} \cdot \mathbf{p}_2)^3}{m_1^2 m_2^2} + 5 \frac{(\mathbf{n}_{12} \cdot \mathbf{p}_1)^3 (\mathbf{n}_{12} \cdot \mathbf{p}_2)^3}{m_1^2 m_2^2} \right] \\ + \frac{G^2 m_1 m_2}{r_{12}^2} \left[\frac{1}{16} (m_1 - 27 m_2) \frac{(\mathbf{p}_1^2)^2}{m_1^2} - \frac{115}{16} m_1 \frac{\mathbf{p}_1^2 (\mathbf{p}_1 \cdot \mathbf{p}_2)}{m_1^2 m_2} + \frac{1}{48} m_2 \frac{25 (\mathbf{p}_1 \cdot \mathbf{p}_2)^2 + 371 \mathbf{p}_1^2 \mathbf{p}_2^2}{m_1^2 m_2^2} \right. \\ \left. + \frac{17 \mathbf{p}_1^2 (\mathbf{n}_{12} \cdot \mathbf{p}_1)^2}{16 m_1^3} - \frac{1}{8} m_1 \frac{(15 \mathbf{p}_1^2 (\mathbf{n}_{12} \cdot \mathbf{p}_2) + 11 (\mathbf{p}_1 \cdot \mathbf{p}_2) (\mathbf{n}_{12} \cdot \mathbf{p}_1)) (\mathbf{n}_{12} \cdot \mathbf{p}_1)}{m_1^2 m_2} + \frac{5 (\mathbf{n}_{12} \cdot \mathbf{p}_1)^4}{12 m_1^3} \right. \\ \left. - \frac{3}{2} m_1 \frac{(\mathbf{n}_{12} \cdot \mathbf{p}_1)^3 (\mathbf{n}_{12} \cdot \mathbf{p}_2)}{m_1^2 m_2} + \frac{125}{12} m_2 \frac{(\mathbf{p}_1 \cdot \mathbf{p}_2) (\mathbf{n}_{12} \cdot \mathbf{p}_1) (\mathbf{n}_{12} \cdot \mathbf{p}_2)}{m_1^2 m_2^2} + \frac{10}{3} m_2 \frac{(\mathbf{n}_{12} \cdot \mathbf{p}_1)^2 (\mathbf{n}_{12} \cdot \mathbf{p}_2)^2}{m_1^2 m_2^2} \right. \\ \left. - \frac{1}{48} (220 m_1 + 193 m_2) \frac{\mathbf{p}_1^2 (\mathbf{n}_{12} \cdot \mathbf{p}_2)^2}{m_1^2 m_2^2} \right] + \frac{G^3 m_1 m_2}{r_{12}^3} \left[-\frac{1}{48} \left(466 m_1^2 + \left(473 - \frac{3}{4} \pi^2 \right) m_1 m_2 + 150 m_2^2 \right) \frac{\mathbf{p}_1^2}{m_1^2} \right. \\ \left. + \frac{1}{16} \left(77 (m_1^2 + m_2^2) + \left(143 - \frac{1}{4} \pi^2 \right) m_1 m_2 \right) \frac{(\mathbf{p}_1 \cdot \mathbf{p}_2)}{m_1 m_2} + \frac{1}{16} \left(61 m_1^2 - \left(43 + \frac{3}{4} \pi^2 \right) m_1 m_2 \right) \frac{(\mathbf{n}_{12} \cdot \mathbf{p}_1)^2}{m_1^2} \right. \\ \left. + \frac{1}{16} \left(21 (m_1^2 + m_2^2) + \left(119 + \frac{3}{4} \pi^2 \right) m_1 m_2 \right) \frac{(\mathbf{n}_{12} \cdot \mathbf{p}_1)(\mathbf{n}_{12} \cdot \mathbf{p}_2)}{m_1 m_2} \right] \\ + \frac{1}{8} \frac{G^4 m_1 m_2^3}{r_{12}^4} \left[\left(\frac{227}{3} - \frac{21}{4} \pi^2 \right) m_1 + m_2 \right] + (1 \leftrightarrow 2). \quad (12)$$

3PN

The EOB Hamiltonian

The effective Hamiltonian (+quartic-in-momenta non-geodesic contribution at 3PN)

$$\hat{H}_{\text{eff}} \equiv \sqrt{p_{r_*}^2 + A \left(1 + \frac{p_\phi^2}{r^2} + z_3 \frac{p_{r_*}^4}{r^2} \right)}$$

$$\frac{dr_*}{dr} = \sqrt{\frac{B}{A}}$$

$$p_{r_*} = \left(\frac{A}{B} \right)^{1/2} p_r$$

The real EOB Hamiltonian of the binary system (from the energy map)

$$\hat{H}^{\text{EOB}} = \frac{1}{\nu} \sqrt{1 + 2\nu \left(\hat{H}_{\text{eff}} - 1 \right)}$$

The Hamiltonian (and the related dynamics) depends, through the “potential” $A(u)$, on the 4PN parameter a_5 . **a_5 is a “free” parameter that needs to be fixed via comparisons with NR simulations.**

$$M = m_1 + m_2$$

$$\nu = m_1 m_2 / (m_1 + m_2)^2$$

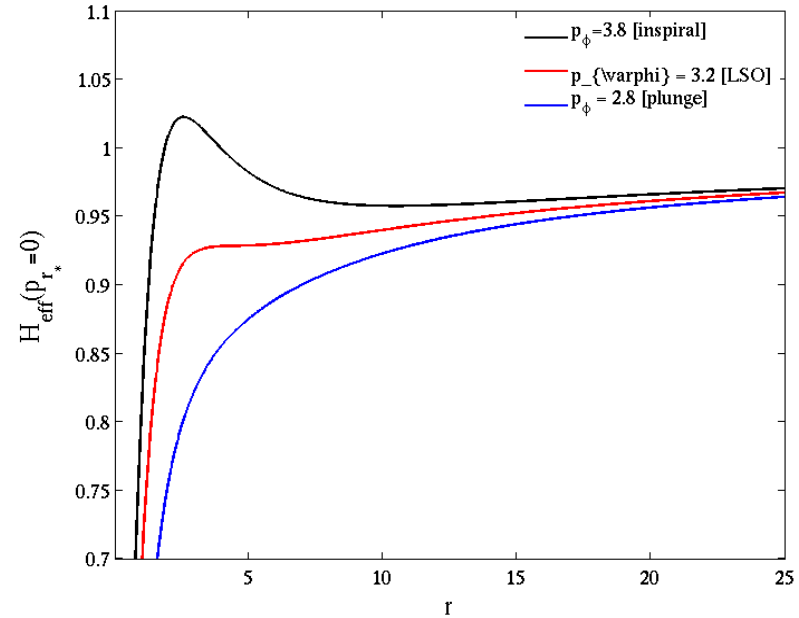
Hamilton's equation + radiation reaction

$$\frac{dr}{dt} = \left(\frac{A}{B}\right)^{1/2} \frac{\partial \hat{H}_{\text{EOB}}}{\partial p_{r_*}},$$

$$\frac{dp_{r_*}}{dt} = -\left(\frac{A}{B}\right)^{1/2} \frac{\partial \hat{H}_{\text{EOB}}}{\partial r},$$

$$\Omega \equiv \frac{d\varphi}{dt} = \frac{\partial \hat{H}_{\text{EOB}}}{\partial p_\varphi},$$

$$\frac{dp_\varphi}{dt} = \hat{\mathcal{F}}_\varphi.$$



Angular momentum loss due to GW emission: start from the PN expression for *radiation reaction* that is explicitly known during the quasi-circular adiabatic inspiral (3.5PN + 4PN correction)

$$\hat{\mathcal{F}}_\varphi^{\text{Taylor}} = -\frac{32}{5} \nu \Omega^5 r_\omega^4 \hat{F}^{\text{Taylor}}(v_\varphi)$$

$$\hat{F}^{\text{Taylor}}(v) = 1 + A_2(\nu) v^2 + A_3(\nu) v^3 + A_4(\nu) v^4 + A_5(\nu) v^5 \\ + A_6(\nu, \log v) v^6 + A_7(\nu) v^7 + A_8(\nu = 0, \log v) v^8$$

Needs resummation of energy flux!

The PN expansions are non-uniformly and non-monotonically convergent in the strong-field regime. One needs to “resum” them in some form in order to extend their validity during the late-inspiral and plunge

- Factorize a simple pole in the GW energy flux
- Resum using near-diagonal Padé approximants (DIS98)

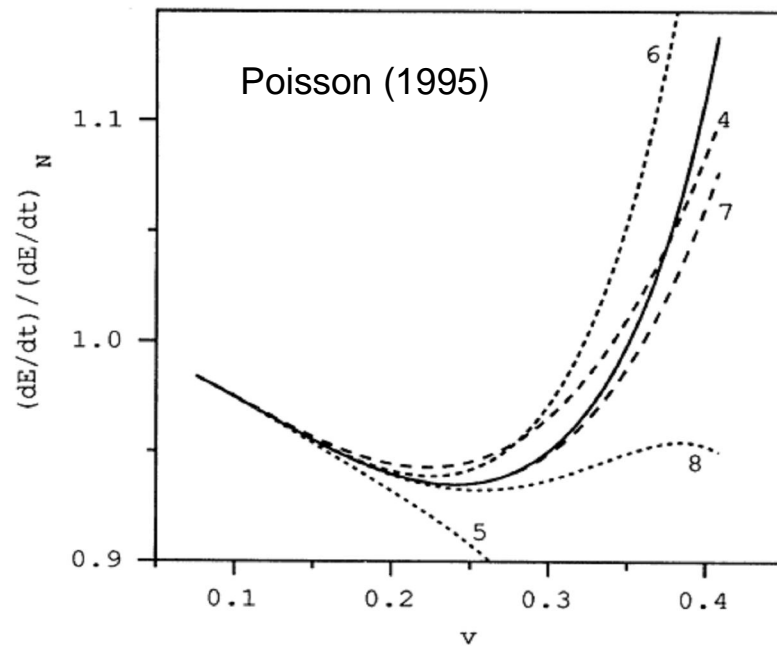


FIG. 1. Various representations of $(dE/dt)/(dE/dt)_N$ as a function of orbital velocity $v = (M/r)^{1/2} = (\pi M f)^{1/3}$. The solid curve represents the exact result $P(v)$, as calculated numerically. The various broken curves represent the post-Newtonian approximations $P_n(v)$, for $n = \{4, 5, 6, 7, 8\}$. The smallest value of v corresponds to an orbital radius r of $175M$; the largest value of v corresponds to $r = 6M$, the innermost stable circular orbit.

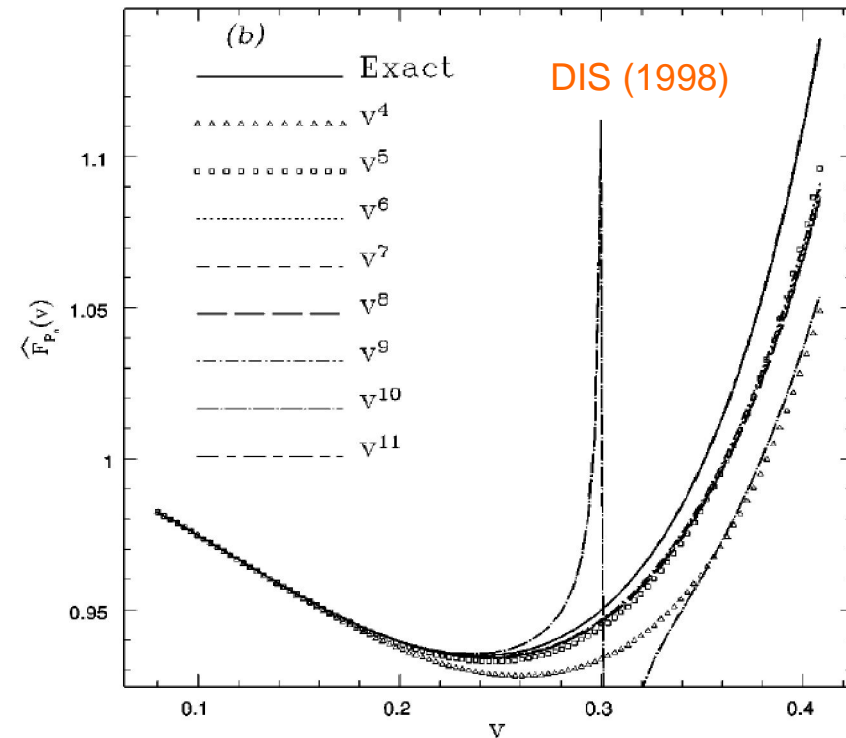


FIG. 3. Newton-normalized gravitational wave luminosity in the test particle limit: (a) T -approximants and (b) P -approximants.

Resumming radiation reaction

Padé resummation of $\hat{\mathcal{F}}_\varphi^{\text{Taylor}} = -\frac{32}{5} \nu \Omega^5 r_\omega^4 \hat{F}^{\text{Taylor}}(v_\varphi)$

- factorize a pole parametrized by v_{pole}
- consider logarithms as coefficients
- use comparable-mass 3.5PN+test-mass 4PN flux
- choose P_4^4 which has no spurious poles
- add non-quasi-circular correction parametrized by a^{RR} [with $\epsilon=0.12$]
- choose argument $v=r\Omega\psi^{1/3}$

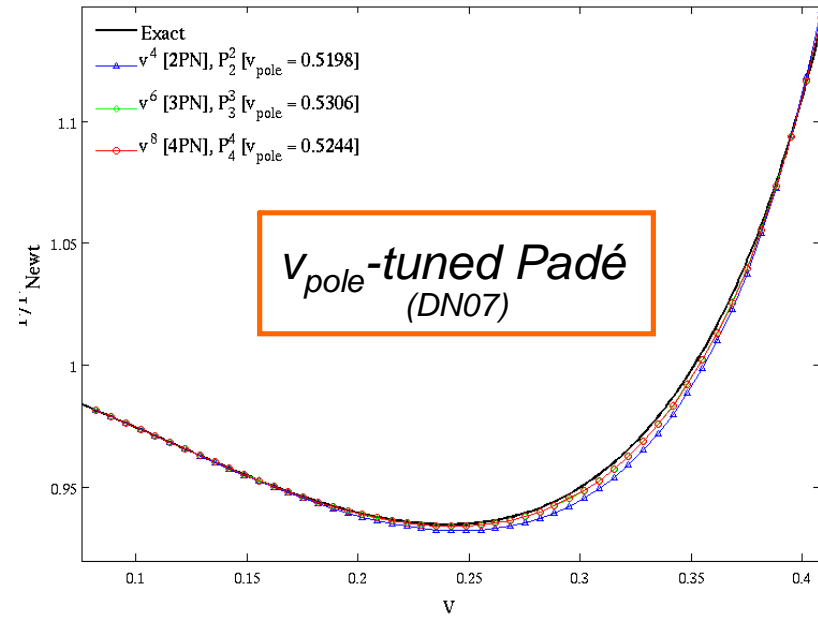
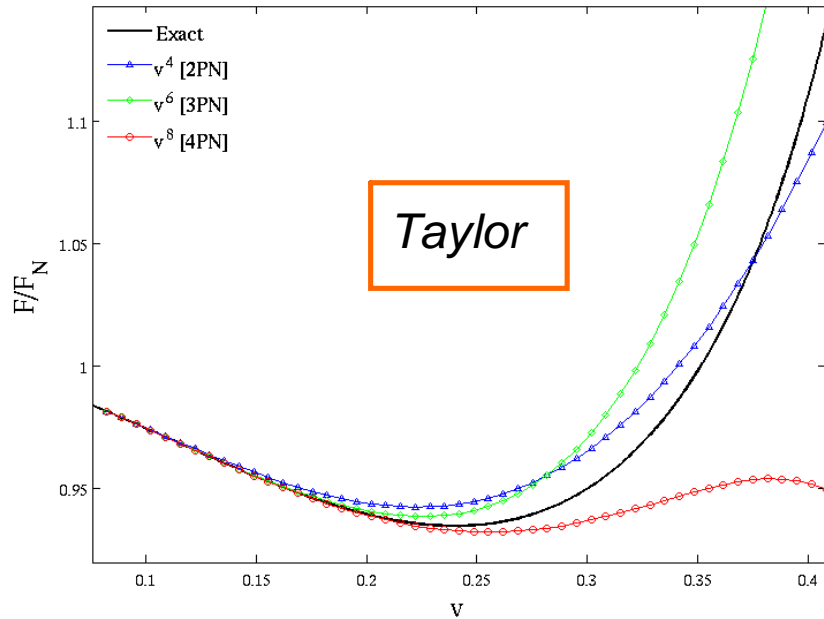
Note prefactor
à la DG06

$$\hat{F}^{\text{resummed}}(v_\varphi) = \left(1 - \frac{v_\varphi}{v_{\text{pole}}}\right)^{-1} P_4^4 \left[\left(1 - \frac{v_\varphi}{v_{\text{pole}}}\right) \hat{F}^{\text{Taylor}}(v_\varphi) \right] \left(1 + \bar{a}^{\text{RR}} \frac{p_{r_*}^2}{(r\Omega)^2 + \epsilon}\right)^{-1}$$

3.5PN + test-mass 4PN contribution

$v_{\text{pole}}, a^{\text{RR}}$ are (in addition to a_5 in H_{EOB})
“free” parameters that need to be fixed
via comparisons with NR simulations.

Comparing Taylor and (tuned) Padé in test-mass case



■ Maximum difference on interval $v < 0.4$:

Taylor(2PN): 0.039
 Taylor(3PN): 0.130
 Taylor(4PN): 0.189

Padé(2PN): 0.0069
 Padé(3PN): 0.0033
 Padé(4PN): 0.0035



Henri Padé, 1863-1953

Resummed EOB *metric* gravitational waveform: inspiral+plunge

- Zerilli-Moncrief normalized (even-parity) waveform (*Real part gives h_+ & imaginary part gives h_x*).
- Multipolar decomposition (expansion on spin-weighted spherical harmonics) here, $l=m=2$.

$$\left(\frac{c^2}{GM}\right) \Psi_{22}^{\text{insplunge}}(t) = -4\sqrt{\frac{\pi}{30}} \nu (r\omega\Omega)^2 f_{22}^{\text{NQC}} F_{22} e^{-2i\Phi}$$

New *PN-resummed (3⁺²PN) correction factor* (DN07a, 07b): 3PN comparable mass + up to 5PN test-mass

$$F_{22}(t) = \hat{H}_{\text{eff}} T_{22} f_{22}(x(t)) e^{i\delta_{22}(t)}$$

- H_{eff} : resums an infinite number of binding energy contributions

$$T_{\ell m} = \frac{\Gamma(\ell + 1 - 2i\hat{k})}{\Gamma(\ell + 1)} e^{\pi\hat{k}} e^{2i\hat{k} \log(2kr_0)}$$

resums an infinite number of leading logarithms in tail effects (both amplitude and phase) obtained from exact solution of Coulomb wave problem

$$f_{22}(x; \nu) = P_2^3 \left[f_{22}^{\text{Taylor}}(x; \nu) \right]$$

Padé-resummed remaining PN-corrected amplitude [flexibility in choice of argument $x(t)$]

- δ_{22} : computed at 3.5PN

Non-quasi-circular corrections to waveform amplitude and phase:

$$f_{22}^{\text{NQC}} = \left[1 + a \frac{p_{r^*}^2}{(r\Omega)^2 + \epsilon} \right] \exp\left(+ib \frac{p_{r^*}}{r\Omega}\right)$$

$b=0$; a is fixed by requiring that the maximum of the modulus of the waveform coincides with the maximum of the orbital frequency

EOB *metric* gravitational waveform: merger and ringdown

EOB approximate representation of the merger (DRT1972 inspired) :

- sudden change of description around the “EOB light-ring” $t=t_m$ (maximum of orbital frequency)
- “match” the insplunge waveform to a superposition of QNMs of the final Kerr black hole
- matching on a 5-teeth comb (*found efficient in the test-mass limit, DN07a*)
- comb of width $7M$ centered on the “EOB light-ring”
- use 5 positive frequency QNMs (found to be near-optimal in the test-mass limit)
- Final BH mass and angular momentum are computed from a fit to NR ringdown (*5 eqs for 5 unknowns*)

$$\Psi_{22}^{\text{ringdown}}(t) = \sum_N C_N^+ e^{-\sigma_N^+ t}$$

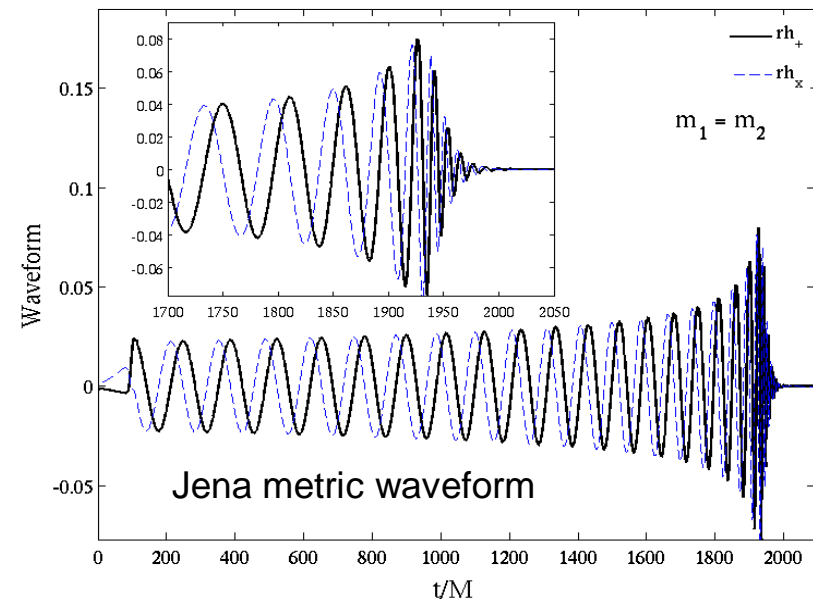
Total EOB waveform covering inspiral-merger and ringdown

$$h_{22}^{\text{EOB}}(t) = \theta(t_m - t) h_{22}^{\text{insplunge}}(t) + \theta(t - t_m) h_{22}^{\text{ringdown}}(t)$$

Accurate EOB-NR comparisons (and calibration)

NR, reduced eccentricity data used (non-spinning black holes only):

- very accurate *inspiral only* data ($m_1=m_2$), 30 GW-cycles *$r\psi_4$ curvature waveform* Caltech-Cornell [Boyle et al. 07] used up to GW frequency 0.1
- Albert-Einstein-Institute, 12 GW-cycles *metric (Zerilli waveform)*, inspiral+merger data ($m_1=m_2$) [DNDPR,08]
- Jena, about 20 GW-cycles *$r\psi_4$ curvature waveform*, inspiral+merger data ($m_1=m_2$; $m_1=2m_2$; $m_1=4m_2$) [DNHBB,08]
- Getting the *metric waveform* by twice integrating the curvature waveform and subtracting linear floors.



1 year ago: Published Caltech-Cornell data to start with...

M. Boyle et al, PRD **76**, 124038 (2007)

- Very accurate NR simulation (without merger) of 1:1 BBH system. About 30 GWs cycles waveform
- Extrapolation in resolution and in extraction radius.
- Thorough comparison with one particular Taylor based 3.5PN approximant. Need to “match” PN at NR waveforms at one particular time.

The TaylorT4 phasing evolution:

$$\frac{dx}{dt} = \frac{16c^3}{5Gm} x^5 \left\{ 1 - \frac{487}{168}x + 4\pi x^{3/2} + \frac{274229}{72576}x^2 - \frac{254}{21}\pi x^{5/2} + \left[\frac{178384023737}{3353011200} + \frac{1475}{192}\pi^2 - \frac{1712}{105}\gamma - \frac{856}{105}\ln(16x) \right] x^3 + \frac{3310}{189}\pi x^{7/2} \right\},$$

$$\frac{d\Phi}{dt} = \frac{x^{3/2}c^3}{Gm}.$$

MICHAEL BOYLE *et al.*

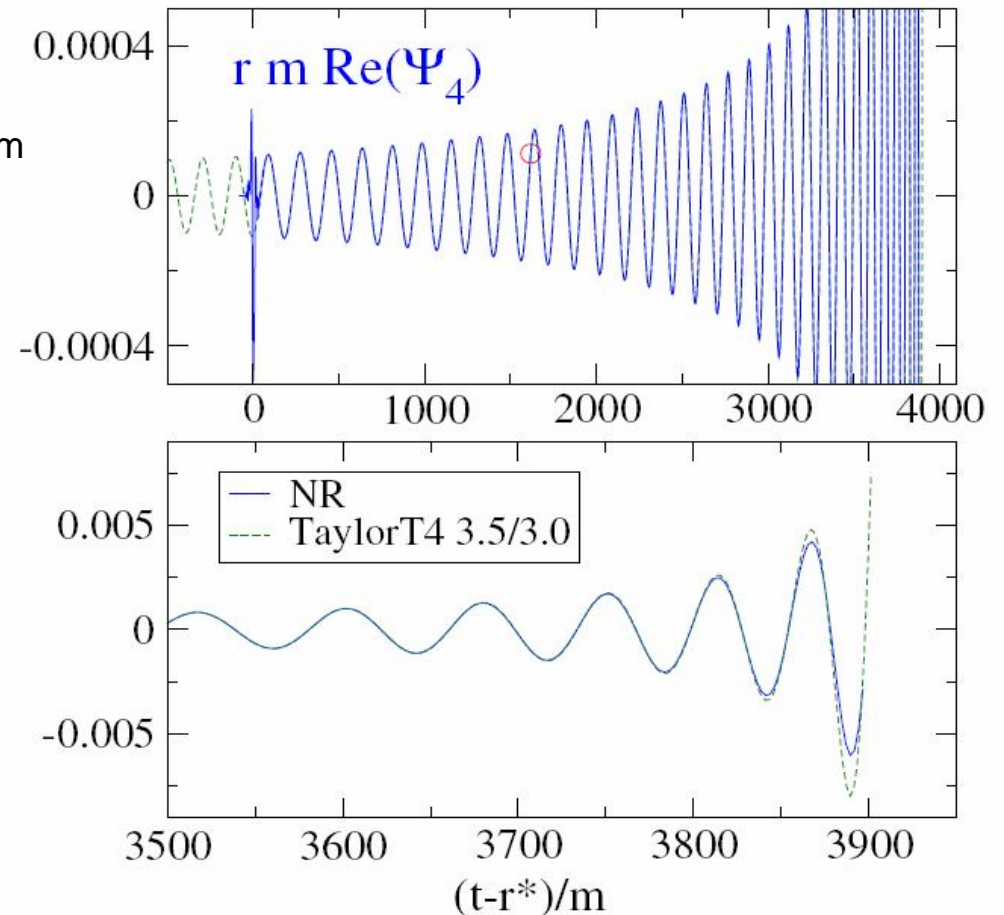


FIG. 20 (color online). Numerical and **TaylorT4 3.5/3.0** waveforms. The PN waveform is matched to the numerical one at $m\omega_m = 0.04$, indicated by the small circle. The lower panel shows a detailed view of the end of the waveform.

1 year ago: Published Caltech-Cornell data to start with...

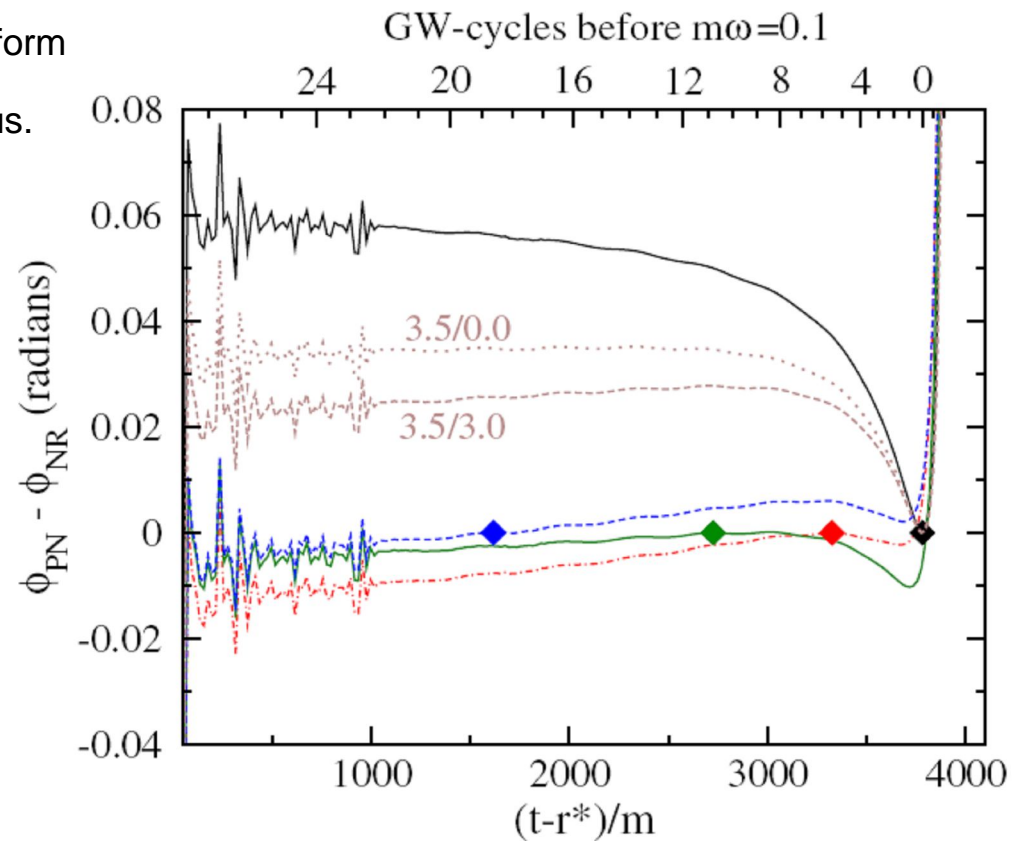
M. Boyle et al, PRD **76**, 124038 (2007)

- Very accurate NR simulation (without merger) of 1:1 BBH system. About 30 GWs cycles waveform
- Extrapolation in resolution and in extraction radius.
- Thorough comparison with one particular Taylor based 3.5PN approximant. Need to “match” PN at NR waveforms at one particular time.

The TaylorT4 phasing evolution:

$$\frac{dx}{dt} = \frac{16c^3}{5Gm} x^5 \left\{ 1 - \frac{487}{168}x + 4\pi x^{3/2} + \frac{274229}{72576}x^2 - \frac{254}{21}\pi x^{5/2} + \left[\frac{178384023737}{3353011200} + \frac{1475}{192}\pi^2 - \frac{1712}{105}\gamma - \frac{856}{105}\ln(16x) \right] x^3 + \frac{3310}{189}\pi x^{7/2} \right\},$$

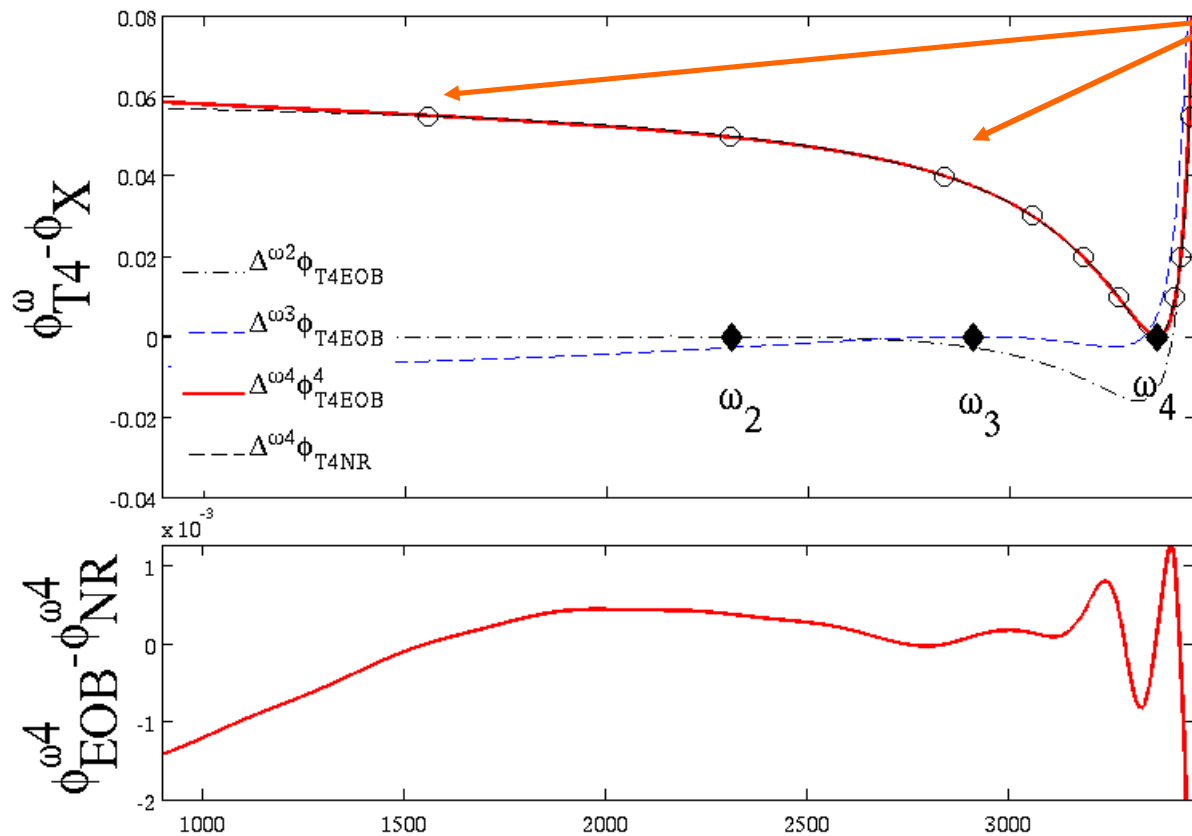
$$\frac{d\Phi}{dt} = \frac{x^{3/2}c^3}{Gm}.$$



Methodology for fitting EOB to NR data

Need to calibrate 3 EOB-flexibility parameters ($a_5, v_{\text{pole}}, a_{\text{RR}}$)

- Use two phase differences [*curvature waveforms*] from published Caltech-Cornell data to have two equations to determine $v_{\text{pole}}(a_5)$ and $a_{\text{RR}}(a_5)$



Impose that the phase Differences T4-EOB and T4-CC agree at these two points

Residual phase difference EOB-NR [*curvature waveforms*]

- Then constrain a_5 by comparing the t phases of EOB and Jena (+AEI) data.

Correlating EOB flexibility parameters

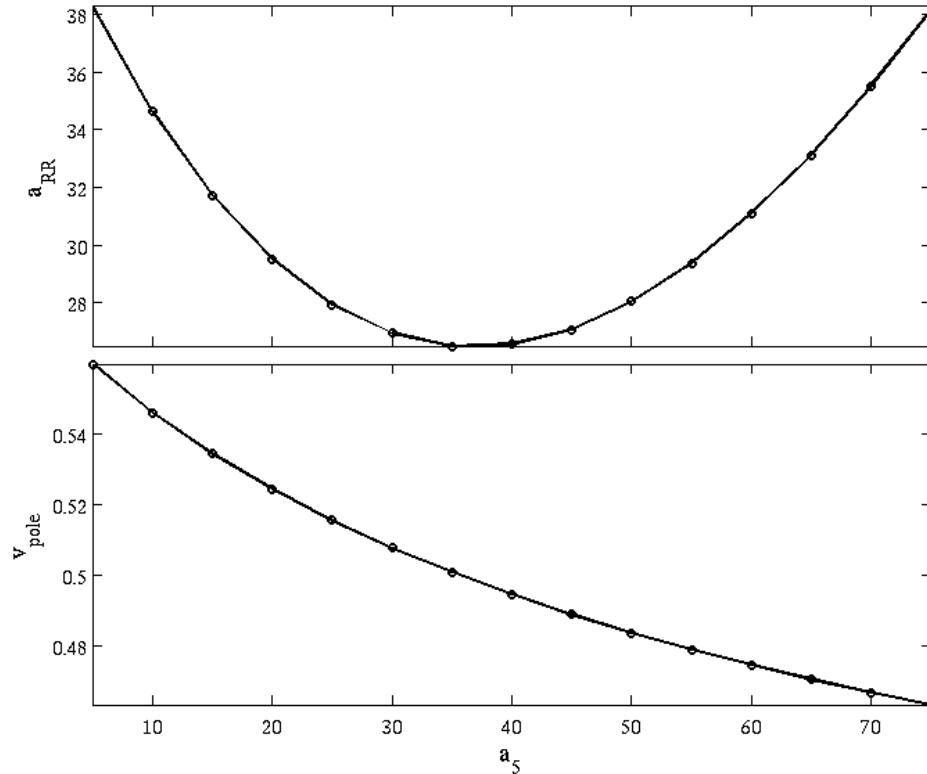


TABLE II: Explicit values of the EOB effective parameters \bar{a}_{RR} and v_{pole} for a certain sample of a_5 . These values correspond to imposing the two constraints $\rho_{\omega_4}^{\delta t_{\omega_4}} \simeq 1 \pm 10^{-4} \simeq \rho_{\omega_4}^{\delta t_{\omega_4}}$.

a_5	\bar{a}_{RR}	v_{pole}
5.0000	38.286713287	0.559878668
10.0000	34.630281690	0.546122851
15.0000	31.708633094	0.534478193
20.0000	29.496402878	0.524422704
25.0000	27.919708029	0.515629404
30.0000	26.940298507	0.507845655
35.0000	26.484962406	0.500903097
40.0000	26.545801527	0.494646066
45.0000	27.057692308	0.488978922
50.0000	28.031496063	0.483798488
55.0000	29.360000000	0.479064301
60.0000	31.097560976	0.474690707
65.0000	33.130252101	0.470660186
70.0000	35.517241379	0.466908044
75.0000	38.189655172	0.463416027

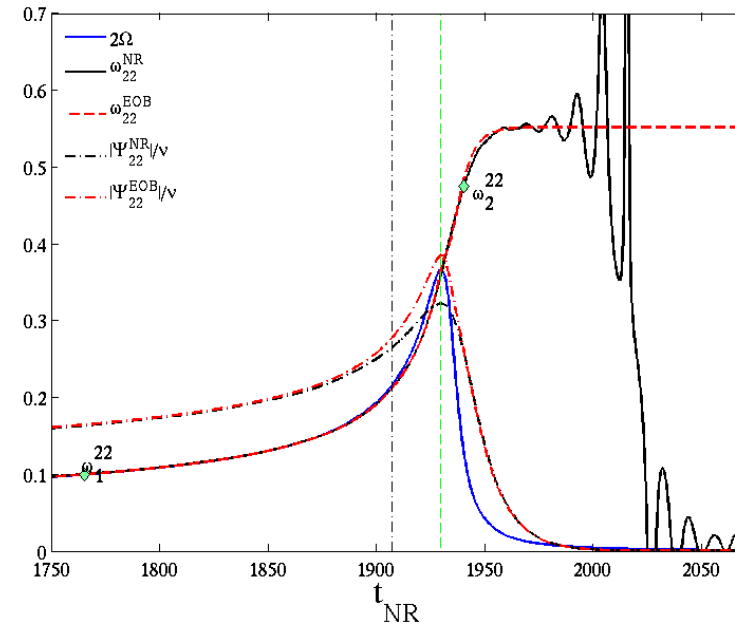
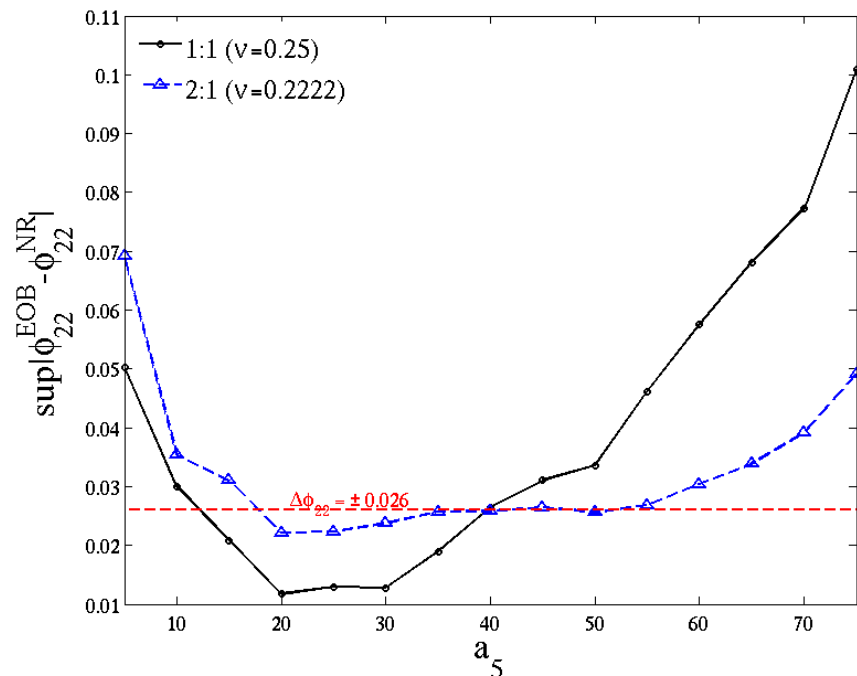
- Use the CC data to express the two free parameters as functions of a_5 .
- Done here with points measured from a published figure. *Checked to be consistent with actual Caltech-Cornell NR data (courtesy of Boyle et al.)*[see later]

Use late-plunge Jena data to constrain the a_5 parameter

Use “plunge and merger” data that are more sensitive to the effect of a_5

Accurate simulations from Jena group for several mass ratios. For 1:1, $D=12$ and 20 GW-cycles waveform. [Double time-integration to get metric waveform]

Diagnostics: L_∞ norm of the [metric waveform] phase difference in the late plunge: from -10.5 to -1.2 GW-cycles before merger, i.e., frequency $0.059 < \omega < 0.19$

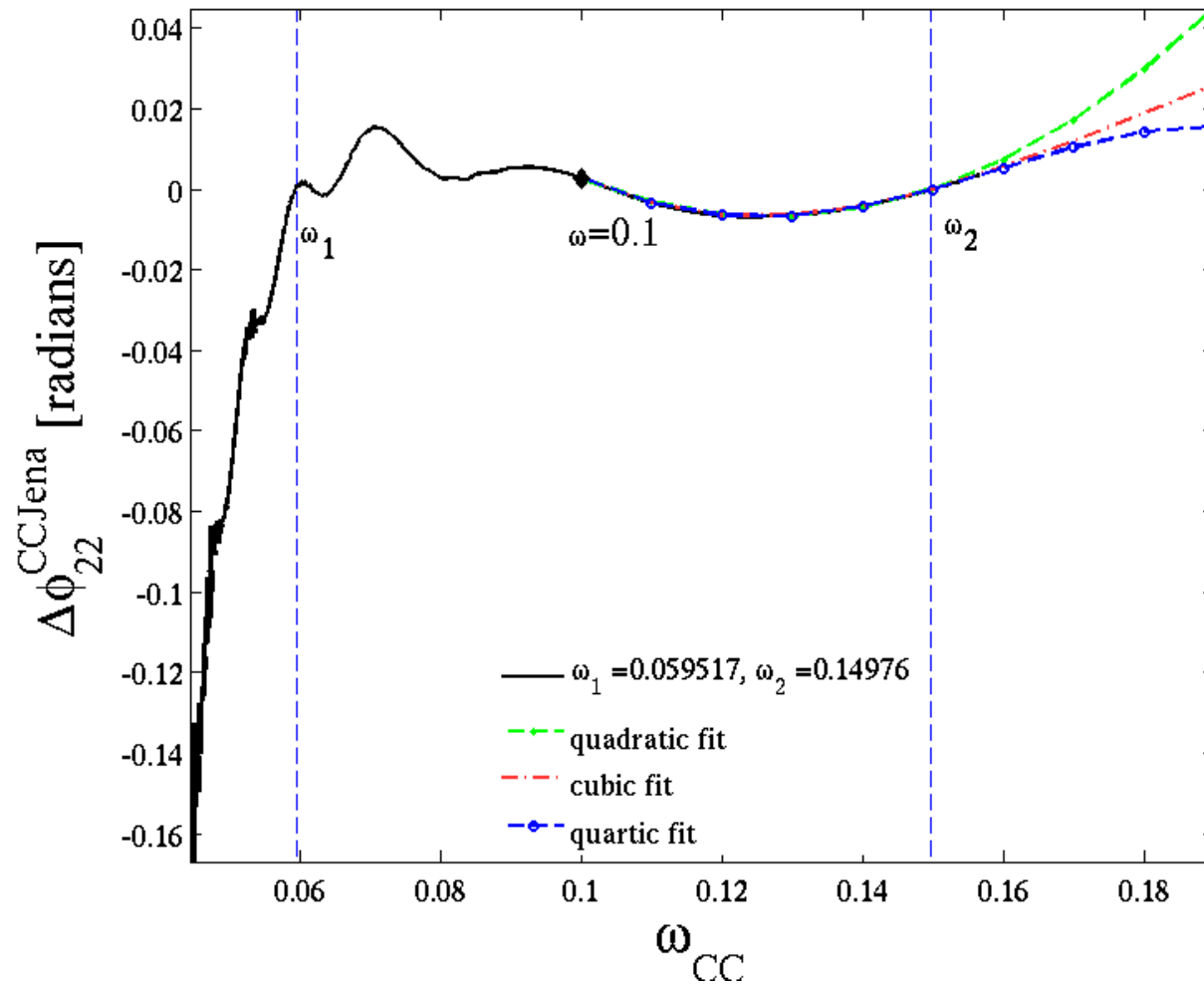


- Presence of a clear minimum (0.01) for the 1:1 mass ratio case
- Consistency with 2:1 mass ratio (where the minimum is more shallow)

current best-bet value: $a_5 \sim 25$

- Range of allowed values of a_5 depending on error level [0.026 radians] in NR data (? $12 < a_5 < 40$?) [see next slide]

Error bars on Jena data (and thus a_5)

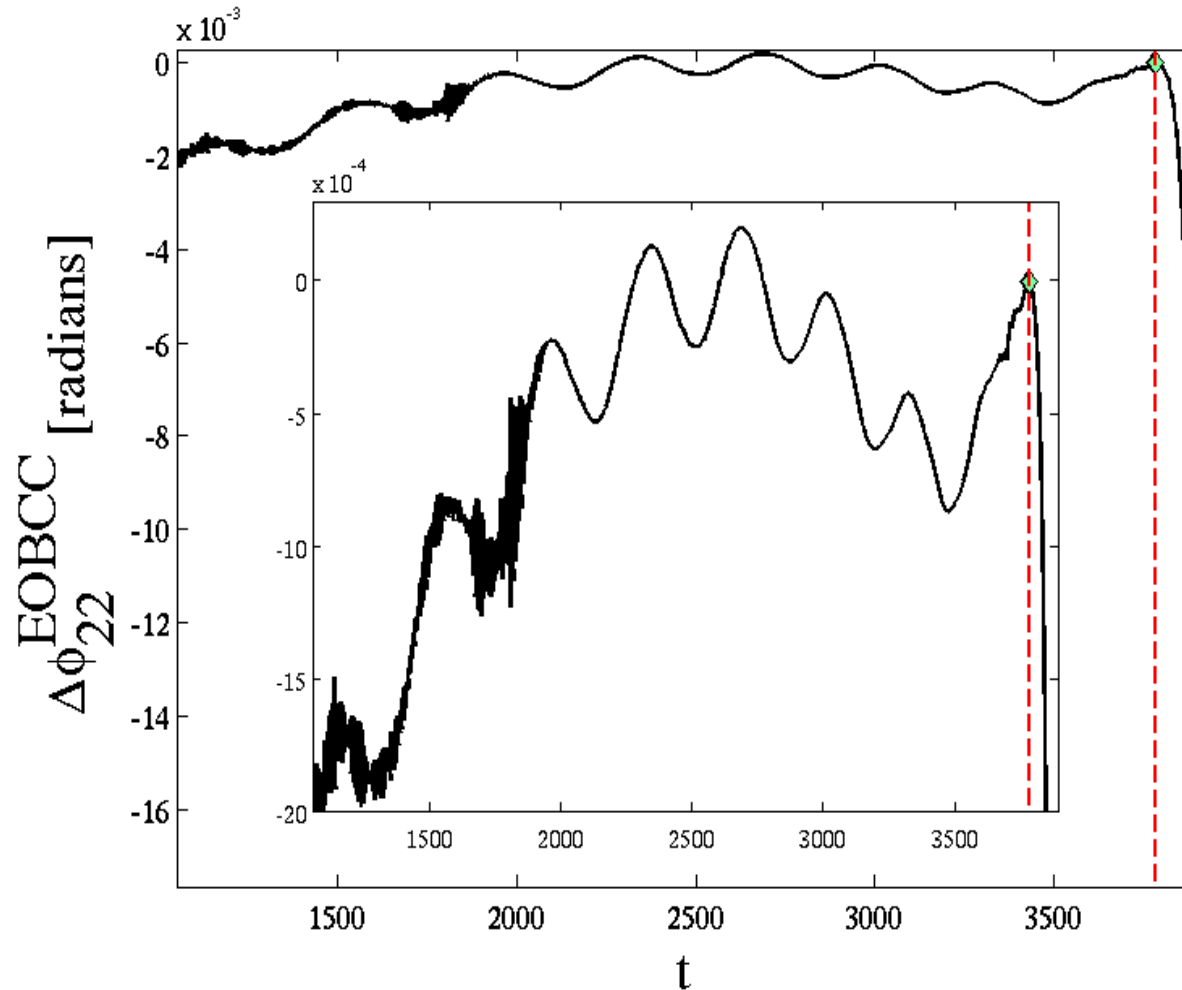


- Errors on Caltech-Cornell data are estimated to be 0.01 radians all over the simulation (Kidder's talk in Jena)

- Estimate errors on Jena data by comparing Jena and Caltech-Cornell data

- Extrapolating in the useful regime $[\omega_L, \omega_R]$, gives ± 0.026 radians

Curvature-waveform **phase difference** EOB-CC (actual data) for $a_5=25$

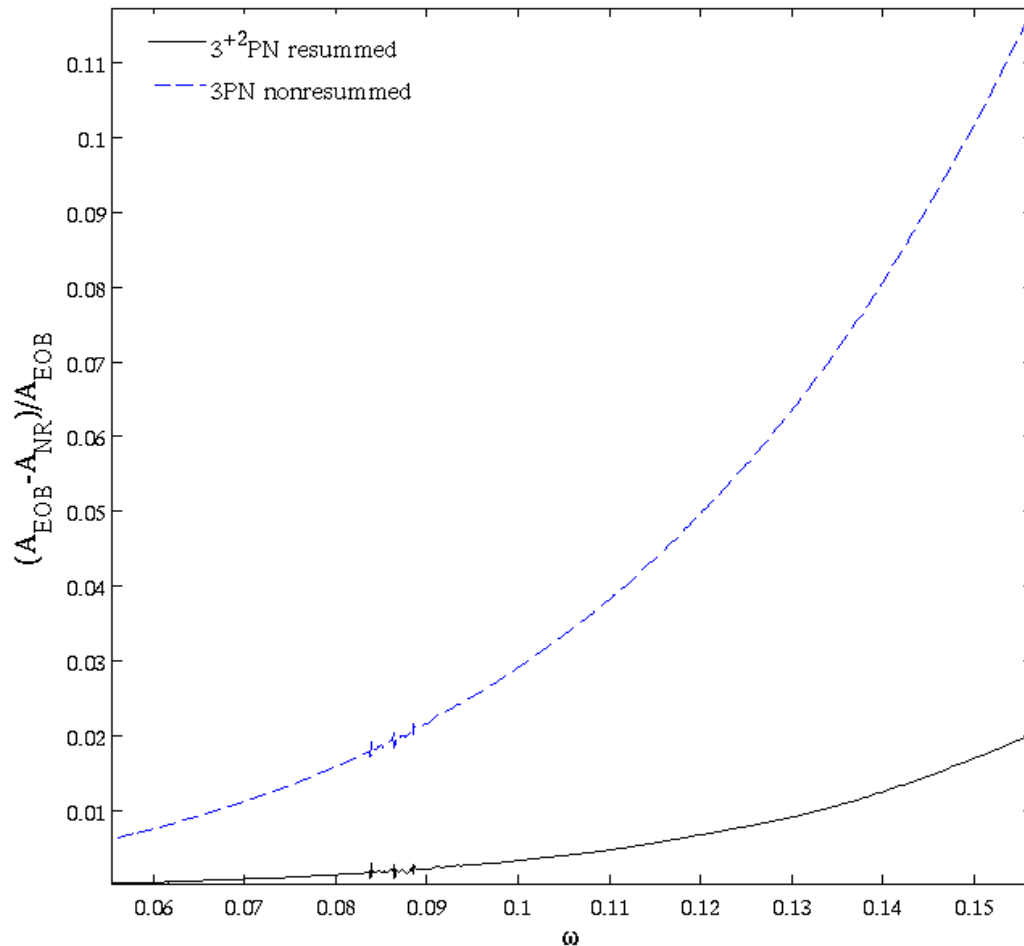


- Close up : maximum phase difference 0.002 radians up to GW frequency 0.1 (OK with DN07b, which used published data)

- Full range: maximum phase difference 0.016 radians accumulated between frequency 0.1 and 0.156

- Two (coincident) “pinching-times” indicated, corresponding to $\omega=0.1$ (the red vertical dashed line)

(Fractional) curvature **amplitude** difference EOB-CC (actual data) for $a_5=25$

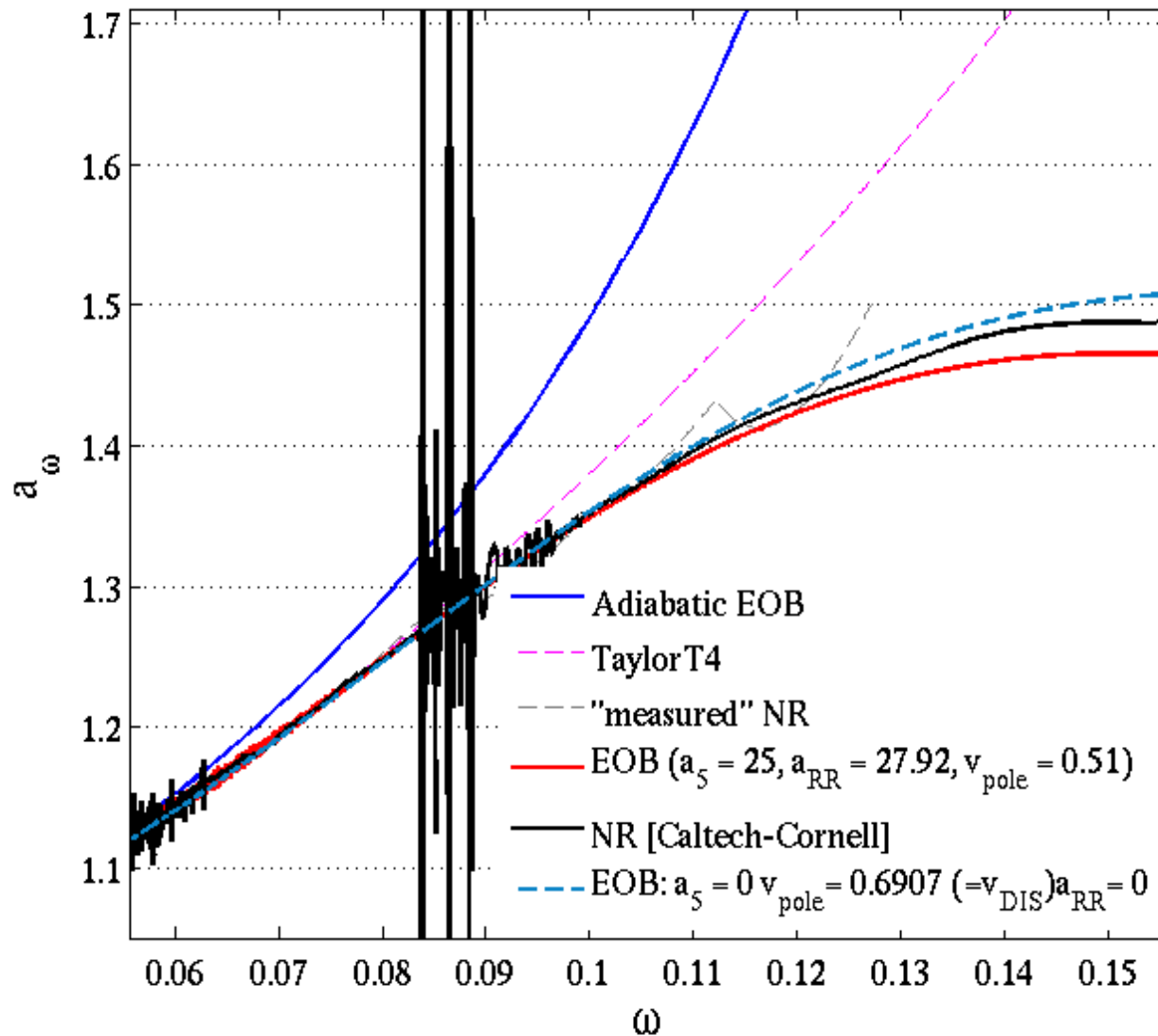


- Nonresummed: fractional differences start at the 1% level and build up to more than 10%

- New resummed EOB amplitude: fractional differences start at the 0.04% level and build up to only 2%

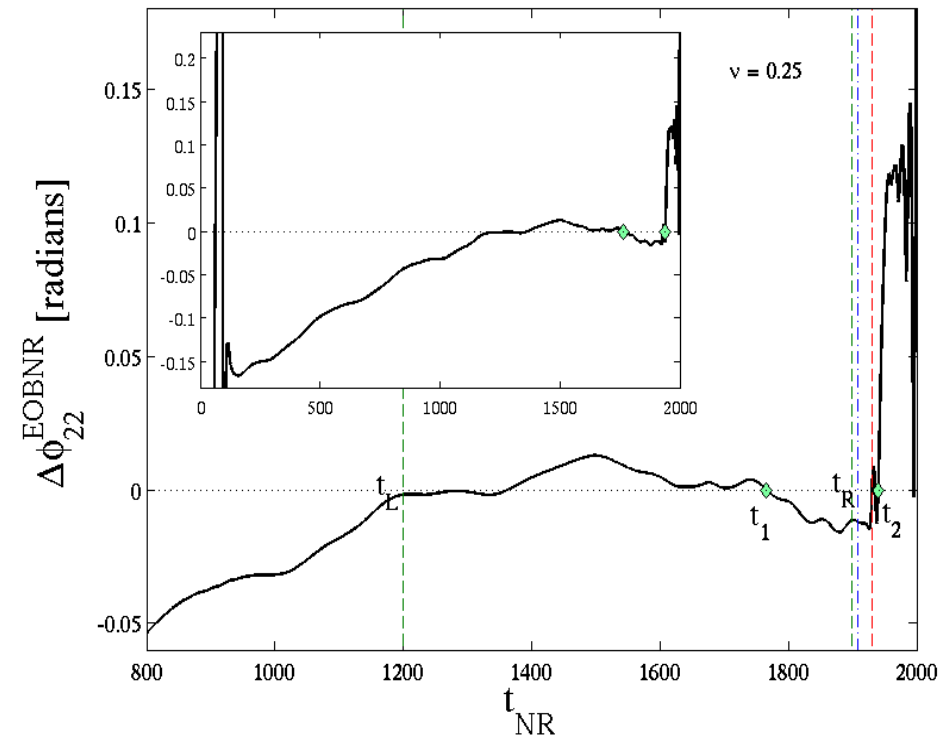
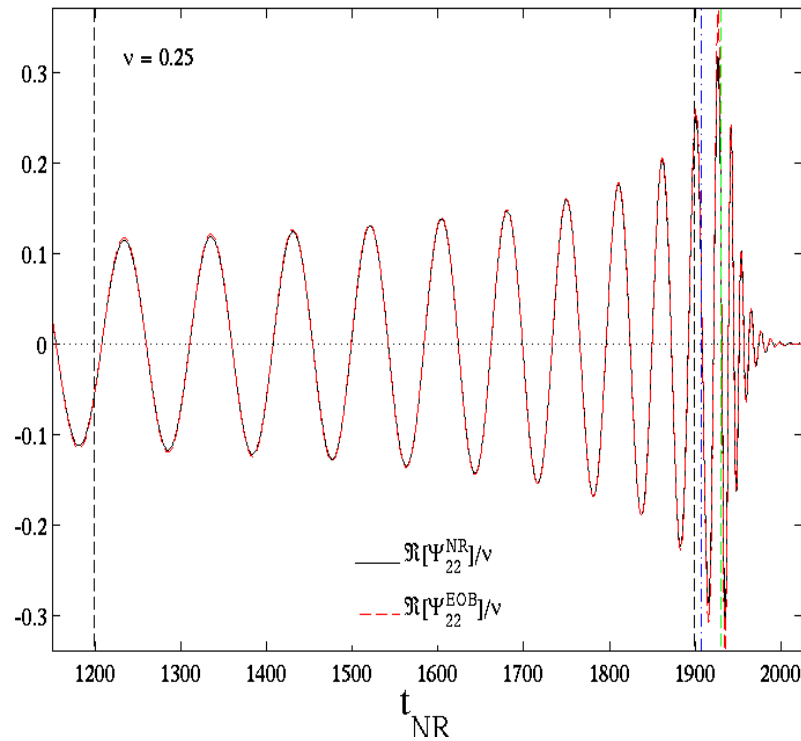
- *Resummation: factor ~20 improvement!*

Comparing $d\omega/dt$ curves: CC (actual data), TaylorT4, adiabatic, untuned and tuned EOB



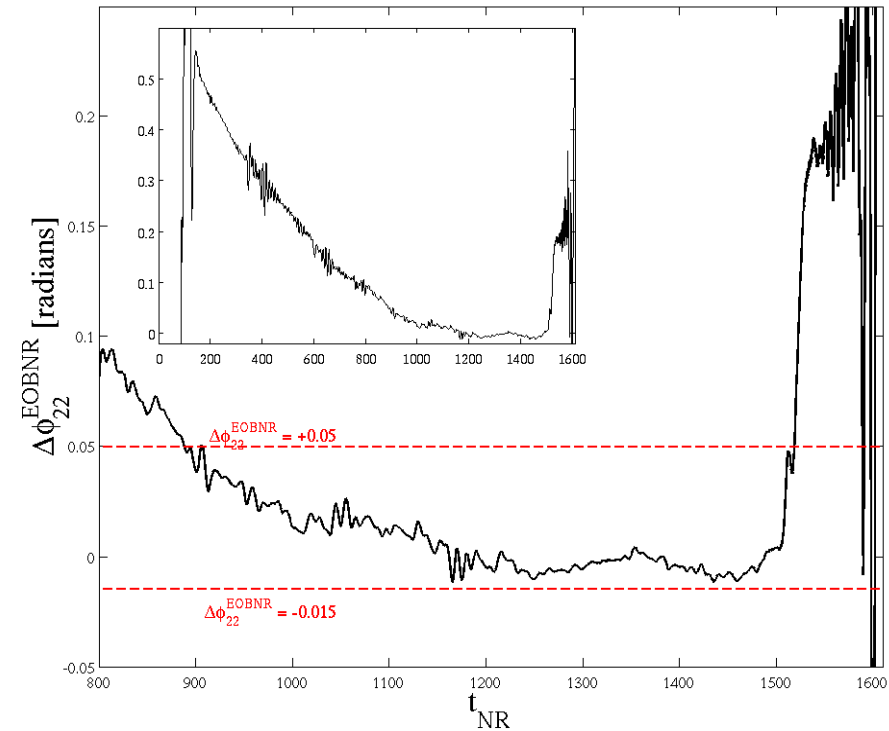
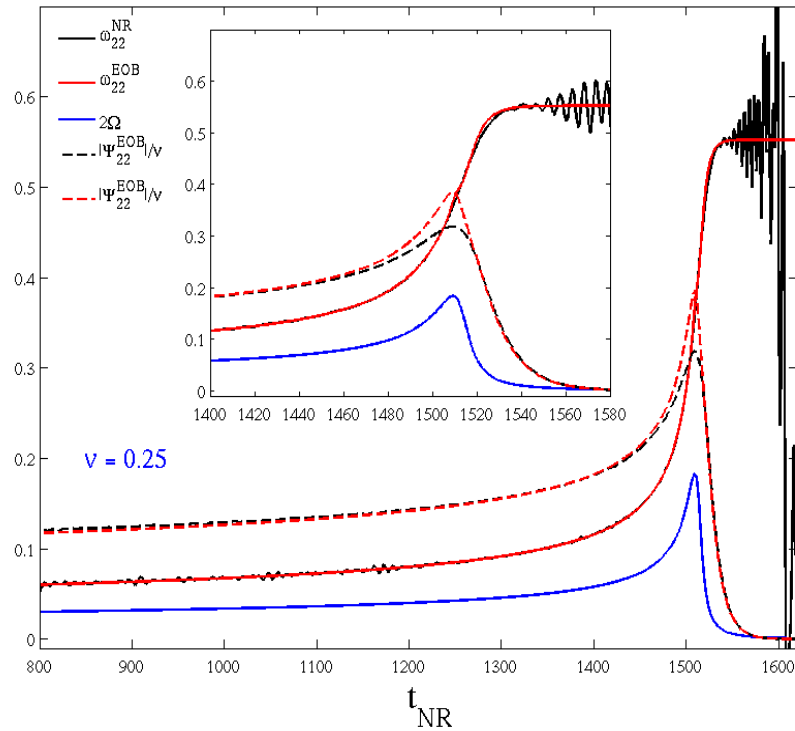
- Here ω is the frequency of the Weyl curvature waveform ψ_4
- Most "intrinsic" curve (OK with DN07b, which used published data)
- Evident presence of nonadiabatic effects [DN07b]
- T4: strongly deviates from NR after GW frequency 0.1

Comparing EOB-NR *metric* waveforms 1:1 case: Jena data



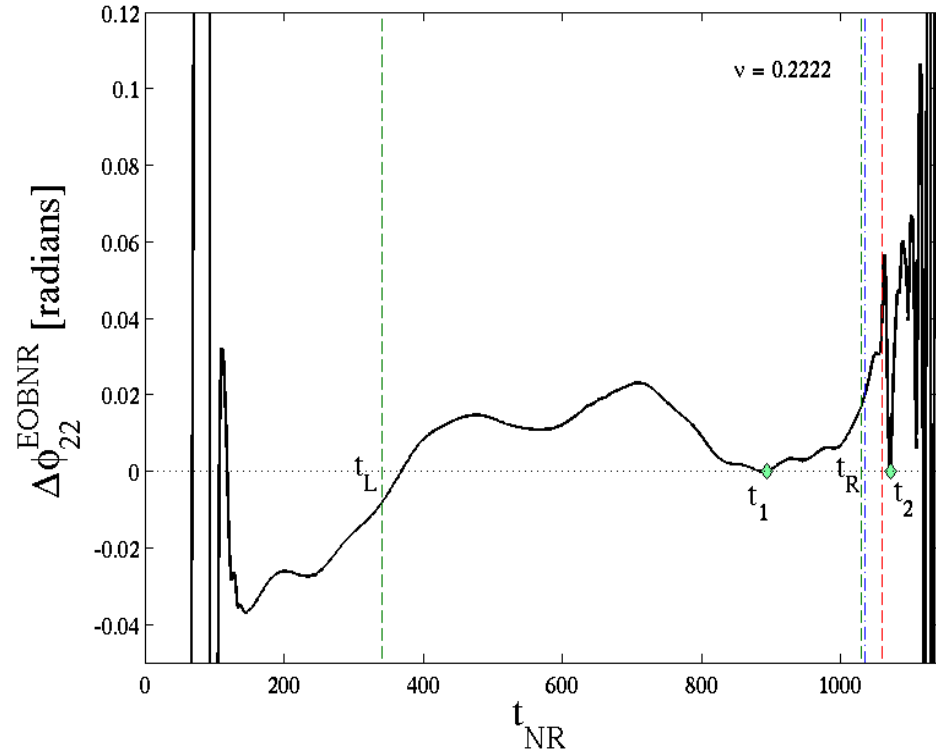
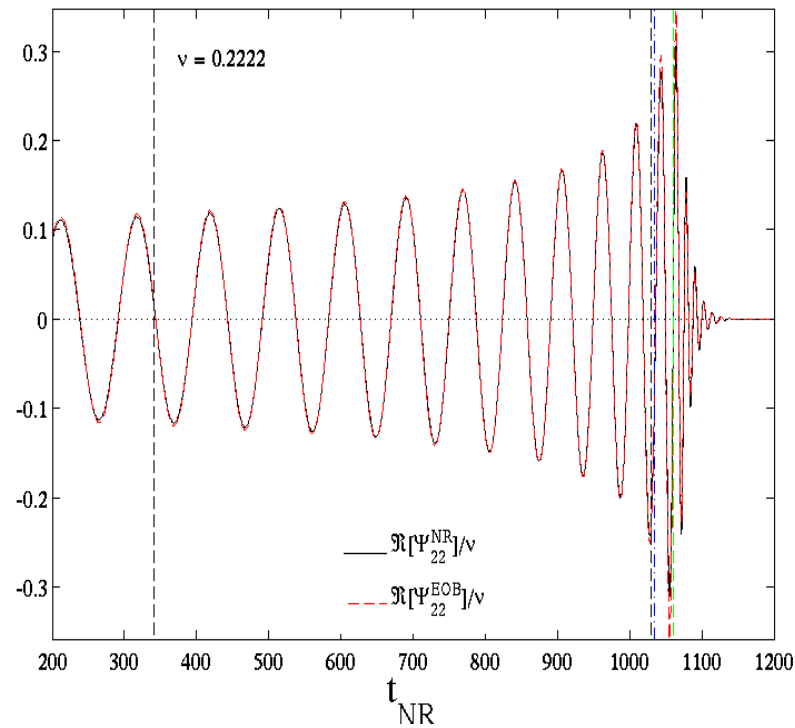
- Metric waveforms from double time-integration of NR curvature waveforms
- $-0.025 < \Delta\phi_{22} < +0.025$ radians ($=0.004$ GW cycles) over 730 M [1200M-1930M]
- At merger, phase jump of only 0.15 radians [$=0.02$ GW cycles].
- We use the same values of flexibility parameters for CC and Jena data: consistency achieved!

Consistency with AEI *metric* waveform 1:1 data



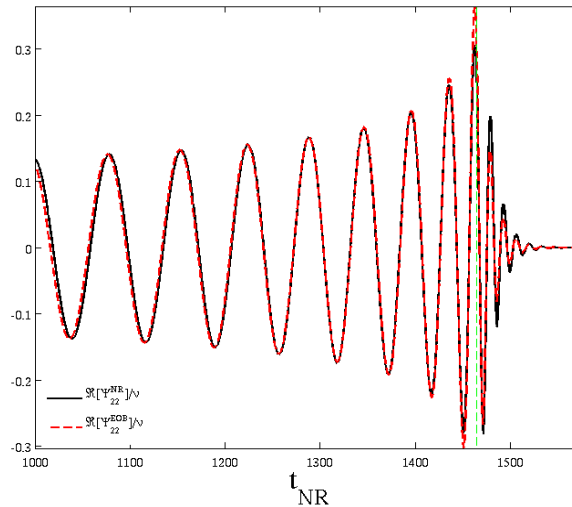
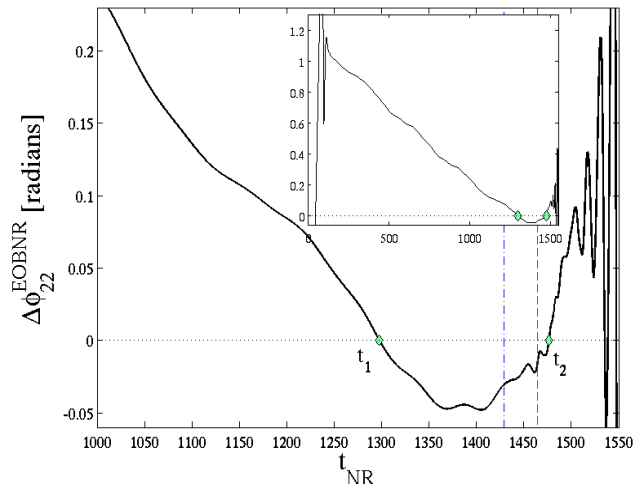
- NR metric waveforms [no need of double time-integration from curvature waveforms]
- $-0.015 < \Delta\phi_{22} < 0.05$ radians (=0.008 GW cycles) over 600M [900M-1500M]
- At merger, phase jumps by 0.18 radians [= 0.028 GW cycles].
- We use the same values of flexibility parameters for CC and AEI data: consistency achieved!

Comparing EOB-NR *metric* waveforms 2:1 case: Jena data



- Metric waveforms from double time-integration of NR curvature waveforms
- $-0.04 < \Delta\phi_{22} < +0.05$ radians (=0.008 GW cycles) over 957M [143M-1100M]
- At merger, phase jump of only 0.06 radians [= 0.009 GW cycles].
- We use the same values of flexibility parameters for CC and Jena data: consistency!

Comparing EOB-NR *metric* waveforms 4:1 case: Jena data



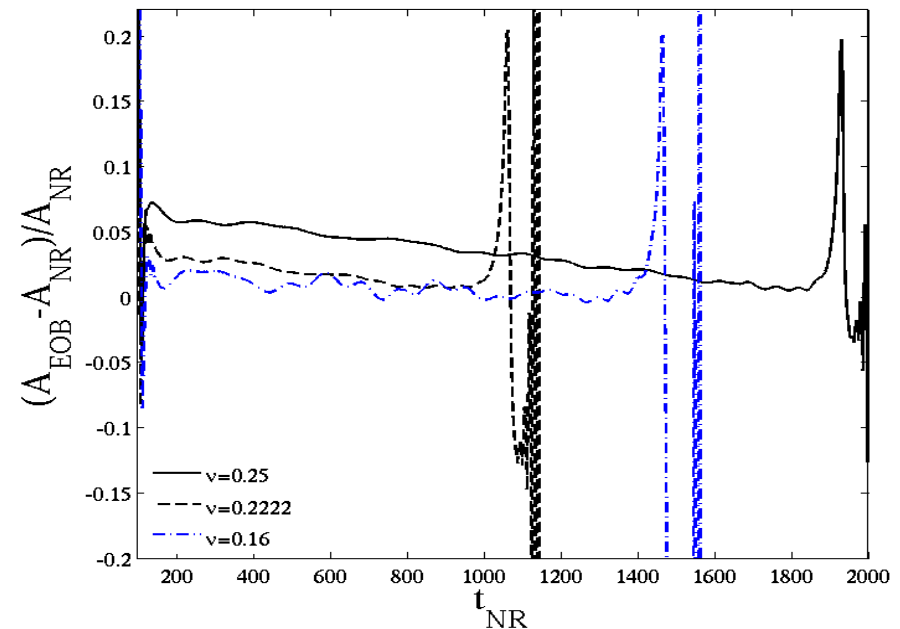
4:1 mass ratio

- Larger accumulated dephasing
- The accuracy of the simulation can be further improved (truncation error is still dominant during the early-inspiral phase)

Comparing EOB-NR *metric* amplitudes: Jena data

Good agreement between the amplitudes:

- Best fractional agreement [equal-mass]: 0.005 during late inspiral
- The NR waves are extracted at finite radius ($r=90M$)
- The agreement improves for smaller ν
- Maximum difference of 20% due to the rather coarse (but still accurate in phasing) matching procedure.



Conclusions

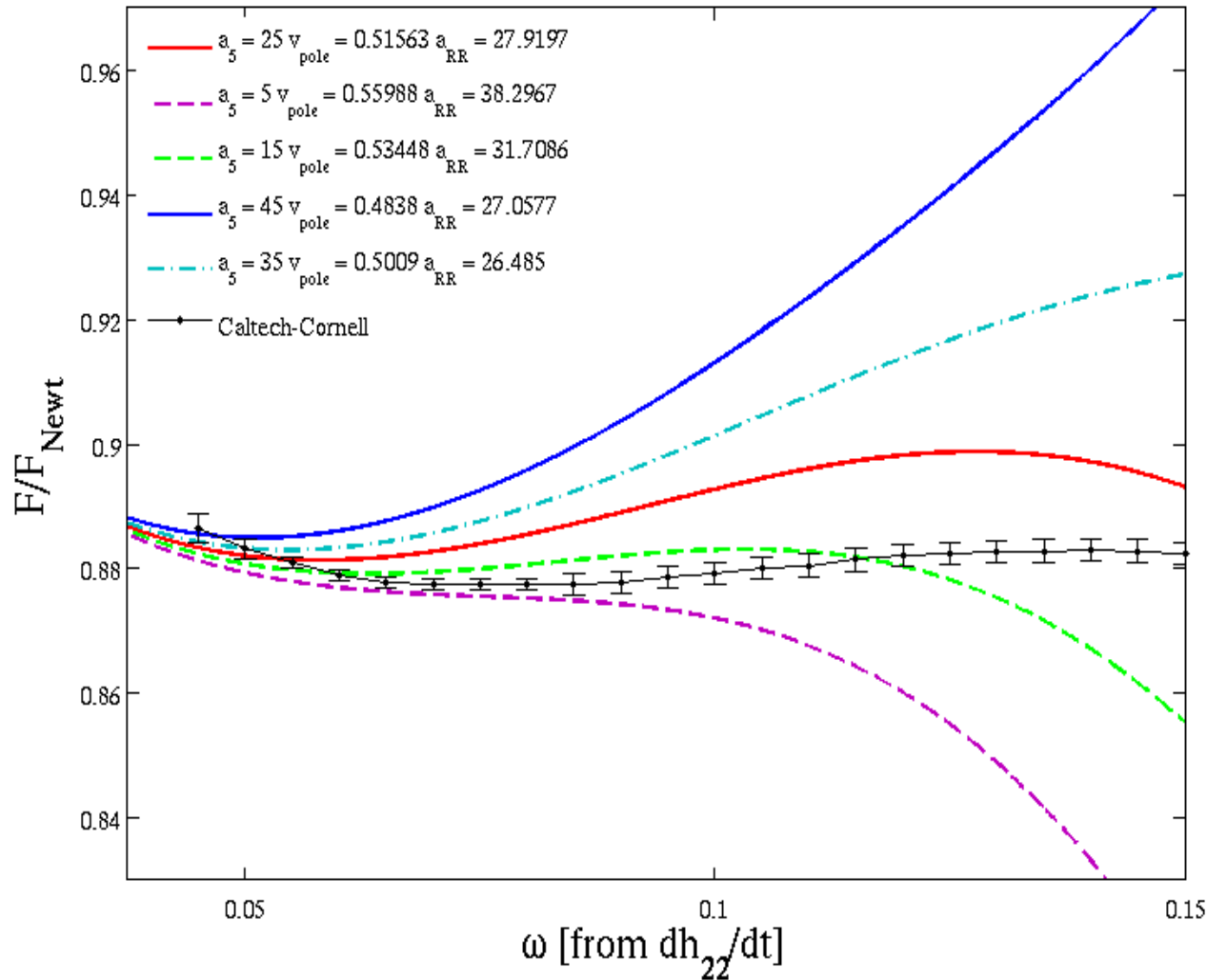
- The EOB formalism made several (qualitative and semi-quantitative) predictions that have been broadly confirmed by NR
- The natural *flexibility* of the EOB parameters leads to a constructive *synergy with NR* results
- The EOB formalism can provide high-accuracy *parameter free* templates $h(m_1, m_2)$ for GWs from BBH coalescence, with unprecedented agreement with NR data, and for any mass ratio.
- Even without using the full flexibility, and without using the resummed 3PN waveform, EOB provides *faithful* templates [Buonanno et al. 2007]
- It is predictive and can give us a physical understanding of dynamics and radiation: energy loss, final spin, recoil,...
- Contrary to the hint of Mroué, Kidder and Teukolsky 2008, that EOB is “only... a very good fitting model”, we think that EOB incorporates a lot of the real physics of coalescing BBH, and that its parametric flexibility is a way to complete it with the “missing” non-perturbative physics provided by NR simulations.

AND

- *Need more comparisons with high-accuracy NR data to better calibrate parameters: collaborations welcome!*
- Quantitatively measuring the effectualness and faithfulness (parameter biases) of new resummed EOB waveforms (*see Buonanno et al. 07 for the restricted EOB waveform*)
- Spinning binaries
- Higher multipoles
- Recoil (see DG06)
- EOB dynamics can help to reduce eccentricity in numerical simulations (as originally suggested BD99,00)

Comparison of (Newton-normalized) EOB and CC energy losses

[*DN2008, preliminary*]



- Published GW energy flux from CC data (black line with error bars) [Boyle, Buonanno et al. 08]
- EOB mechanical energy losses, $-dH/dt$ (coloured lines)
- Confirms the approximate range of a_5 values
- Extends its validity to GW frequencies above 0.1